without mismatches were aligned to the same regions using SHRiMP2.2.2[42]. SHRiMP2.2.2 seeds were set based on the length of the read allowing 1 mismatch anywhere in the body and up to 3 mismatches at the 3′ end of the read (based on the length of the read). (Figure 1a right, Figure 2b, Supplemental Figure 7, Supplemental Table 4). *Small RNA-sequencing data was deposited on GEO (GSE57381).*

AGO2-RNA Co-immunoprecipitation. FT3-7 cells were grown in Dulbecco's modified Eagle's medium (DMEM, Life Technologies) and supplemented with 10% fetal calf serum and 2 mM GlutaMAX (Life Technologies, Carlsbad, CA). Cells were cultured in a humidified incubator at 37°C and 5% CO_2. Three technical replicates of 1×10^7 FT3-7 cells were harvested in lysis buffer [150 mM KCl, 25 mM Tris-HCl (pH 7.4), 5 mM EDTA, 1% Triton X-100, 5 mM DTT, Complete protease inhibitor mixture (Roche), and 100 U/mL RNaseOUT (Life Technologies)]. Lysates were centrifuged for 30 min at 17,000 × g at 4°C and filtered through a 0.22-um filter. Filtrates were incubated with anti-human AGO2 mAb (RN003M, MBL International, Woborn, MA) or isotype control IgG (Abcam, Cambridge, England) at 4°C for 2 h, followed by addition of 30 μL of Protein G Sepharose (GE Healthcare) for 1 h. The Sepaharose beads were washed three times in lysis buffer and RNA extracted using the miRNeasy Mini Kit (Qiagen, Hilden, Germany).

Small RNA real time quantitative PCR (RT-qPCR). Complementary DNA (cDNA) was synthesized using TaqMan MicroRNA Reverse Transcription Kit (Life Technologies) according to the manufacturer's instructions. Real time PCR amplification was performed using TaqMan Universal Master Mix (Life Technologies) on the Bio-Rad CFX96 real time PCR detection system. *U6*, miR-24, let-7a, let-7f, *RNU48*, and *RNU66* were all evaluated as potential housekeeping small RNAs for purposes of normalization. *RNU48* was selected because it was the most consistent across disease groups. RT-qPCR reactions for human samples were performed in triplicate. RT-qPCR reactions for chimpanzee samples were performed in duplicate. The following TaqMan assays were purchased from Life Technologies: miR-122 (product number 4427975; 002245) and *RNU48* or *SNORD48* (product number 4427975; 001006). Primers for the custom TaqMan assays (5′ tRH-^{Gly} and 5′ tRH-^{Val}) were designed using 5′-GCAUUGGUGGUUCAGUGGUAGAAU-UCUCGCCU-3′ for 5′ tRH-^{Gly} and 5′-GUUUCCGUAGUGUAGUGGUUAUCAC-GUUCGCCU-3′ for 5′ tRH^{Val}.

Metabolic Radiolabeling and Measurement of Nascent Protein Synthesis. Huh7 cells were seeded onto the wells of 6-well cell culture plates at a density of 2×10^5 cells/well and incubated overnight to allow cell attachment. Cells were transfected with 50 nM and 100 nM of 5′ tRH^{Gly} (5′-GCAUUGGUGGUUCAGUGGUAGAAU-UCUCGCCU-3′), 5′ tRH^{Val} (5′-GUUUCCGUAGUGUAGUGGUUAUCACGUU-CGCCU-3′), or scramble (5′-GCAUUCACUUGGAUAGUAAAUCCAAGC-UGAA-3′)[21] (all from Integrated DNA Technologies, Coralville, IA) oligonucleotide after replacing cell culture medium with methionine- and cysteine-deficient DMEM (Life Technologies) and cultured for further 12 hrs. Cells were then metabolically radiolabeled for 12 hrs with 200 μCi/well of Express Protein Labeling Mix containing [^{35}S]methionine and [^{35}S]cysteine (PerkinElmer, Waltham, MA) in the presence or absence of 50 μg/ml puromycin and lysed with lysis buffer (20 mM Tris-HCl [pH 7.4] containing 150 mM NaCl, 1% Triton X-100, 0.05% SDS, and 10% glycerol) supplemented with 50 mM NaF, 5 mM Na_3VO_4, and a protease inhibitor cocktail (Complete; Roche, Mannheim, Germany). The protein concentration of cell lysates was determined by the Bio-Rad Protein Assay (Bio-Rad), and 10 μg (total protein) of cell lysates was subjected to SDS-PAGE followed by staining gels with the Sypro Ruby Protein Gel Stain (Bio-Rad, Hercules, CA) and autoradiography.

Immunohistochemistry (IHC). Staining was performed by immunoperoxidase technique with an Envision kit (DAKO Japan). Primary antibodies used were against β-actin (Cell signaling technology, #4967, Beverly, MA) and Human Angiogenin Affinity Purified Polyclonal Ab (R and D Systems, AF265, Minneapolis, MN).

1. Arzumanyan, A., Reis, H. M. & Feitelson, M. A. Pathogenic mechanisms in HBV- and HCV-associated hepatocellular carcinoma. *Nat Rev Cancer* **13**, 123–135 (2013).
2. Perz, J. F., Armstrong, G. L., Farrington, L. A., Hutin, Y. J. & Bell, B. P. The contributions of hepatitis B virus and hepatitis C virus infections to cirrhosis and primary liver cancer worldwide. *J Hepatol* **45**, 529–538 (2006).
3. Hou, W. & Bonkovsky, H. L. Non-coding RNAs in hepatitis C-induced hepatocellular carcinoma: dysregulation and implications for early detection, diagnosis and therapy. *World J Gastroenterol* **19**, 7836–7845 (2013).
4. Xu, X. *et al.* Hepatitis B virus X protein represses miRNA-148a to enhance tumorigenesis. *J Clin Invest* **123**, 630–645 (2013).
5. Chen, Y. *et al.* HCV-induced miR-21 contributes to evasion of host immune system by targeting MyD88 and IRAK1. *PLoS Pathog* **9**, e1003248 (2013).
6. Jopling, C. L., Yi, M., Lancaster, A. M., Lemon, S. M. & Sarnow, P. Modulation of hepatitis C virus RNA abundance by a liver-specific MicroRNA. *Science* **309**, 1577–1581 (2005).
7. Shimakami, T. *et al.* Stabilization of hepatitis C virus RNA by an Ago2-miR-122 complex. *Proc Natl Acad Sci U S A* **109**, 941–946 (2012).
8. Janssen, H. L. *et al.* Treatment of HCV Infection by Targeting MicroRNA. *N Engl J Med* **368**, 1685–1694 (2013).
9. Garcia-Silva, M. R., Cabrera-Cabrera, F. & Güida, M. C. Hints of tRNA-Derived Small RNAs Role in RNA Silencing Mechanisms. *Genes* **3**, 603–614 (2012).
10. Wang, Q. *et al.* Identification and functional characterization of tRNA-derived RNA fragments (tRFs) in respiratory syncytial virus infection. *Mol Ther* **21**, 368–379 (2013).
11. Gong, B. *et al.* Compartmentalized, functional role of angiogenin during spotted fever group rickettsia-induced endothelial barrier dysfunction: evidence of possible mediation by host tRNA-derived small noncoding RNAs. *BMC Infect Dis* **13**, 285 (2013).
12. Saikia, M. *et al.* Angiogenin-Cleaved tRNA Halves Interact with Cytochrome c Protecting Cells from Apoptosis during Osmotic Stress. *Mol Cell Biol* **34**, 2450–63 (2014).
13. Hou, J. *et al.* Identification of miRNomes in human liver and hepatocellular carcinoma reveals miR-199a/b-3p as therapeutic target for hepatocellular carcinoma. *Cancer Cell* **2**, 232–243 (2011).
14. Spaniel, C., Honda, M., Selitsky, S. R. & Yamane, D. microRNA-122 abundance in hepatocellular carcinoma and non-tumor liver tissue from Japanese patients with persistent HCV versus HBV infection. *PloS One* **8**, e76867 (2013).
15. Bartel, D. P. MicroRNAs: target recognition and regulatory functions. *Cell* **136**, 215–233 (2009).
16. Chan, P. P. & Lowe, T. M. GtRNAdb: a database of transfer RNA genes detected in genomic sequence. *Nucleic Acids Res* **37**, D93–97 (2009).
17. Kozomara, A. & Griffiths-Jones, S. miRBase: annotating high confidence microRNAs using deep sequencing data. *Nucleic Acids Res* **42**, D68–73 (2014).
18. Lanford, R. E., Lemon, S. M. & Walker, C. in *Hepatitis C Antiviral Drug Discovery & Development* (eds He, Y. & Tan, T.) 99–132 (Horizons Scientific Press, 2011).
19. Asabe, S. *et al.* The size of the viral inoculum contributes to the outcome of hepatitis B virus infection. *J Virol* **83**, 9652–9662 (2009).
20. Fu, H. *et al.* Stress induces tRNA cleavage by angiogenin in mammalian cells. *FEBS Lett* **583**, 437–442 (2009).
21. Yamasaki, S., Ivanov, P., Hu, G.-F. & Anderson, P. Angiogenin cleaves tRNA and promotes stress-induced translational repression. *J Cell Biol* **185**, 35–42 (2009).
22. Wang, Q. *et al.* Identification and functional characterization of tRNA-derived RNA fragments (tRFs) in respiratory syncytial virus infection. *Mol Ther* **21**, 368–379 (2013).
23. Gong, B. *et al.* Compartmentalized, functional role of angiogenin during spotted fever group rickettsia-induced endothelial barrier dysfunction: evidence of possible mediation by host tRNA-derived small noncoding RNAs. *BMC Infect Dis* **13**, 285 (2013).
24. Mishima, E. *et al.* Conformational Change in Transfer RNA Is an Early Indicator of Acute Cellular Damage. *J Am Soc Nephrol* **25**, 2316–26 (2014).
25. Ivanov, P., Emara, M. M., Villen, J., Gygi, S. P. & Anderson, P. Angiogenin-induced tRNA fragments inhibit translation initiation. *Mol Cell* **43**, 613–623 (2011).
26. Emara, M. M. *et al.* Angiogenin-induced tRNA-derived stress-induced RNAs promote stress-induced stress granule assembly. *J Biol Chem* **285**, 10959–10968 (2010).
27. Dhahbi, J. M. *et al.* 5′ tRNA halves are present as abundant complexes in serum, concentrated in blood cells, and modulated by aging and calorie restriction. *BMC Genomics* **14**, 298 (2013).
28. Vojtech, L. *et al.* Exosomes in human semen carry a distinctive repertoire of small non-coding RNAs with potential regulatory functions. *Nucleic Acids Res* **42**, 7290–7304 (2014).
29. Garcia-Silva, M. R. *et al.* Gene Expression Changes Induced by Trypanosoma cruzi Shed Microvesicles in Mammalian Host Cells: Relevance of tRNA-Derived Halves. *Biomed Res Int* **2014**, 305239 (2014).
30. Fu, H. *et al.* Stress induces tRNA cleavage by angiogenin in mammalian cells. *FEBS Lett* **583**, 437–442 (2009).
31. Yamasaki, S., Ivanov, P., Hu, G.-F. & Anderson, P. Angiogenin cleaves tRNA and promotes stress-induced translational repression. *J Biol Chem* **185**, 35–42 (2009).
32. Gao, X. & Xu, Z. Mechanisms of action of angiogenin. *Acta Biochim Biophys Sin (Shanghai)* **40**, 619–624 (2008).
33. Pizzo, E. *et al.* Ribonuclease/angiogenin inhibitor 1 regulates stress-induced subcellular localization of angiogenin to control growth and survival. *J Cell Sci* **126**, 4308–4319 (2013).
34. Saxena, S. K., Rybak, S. M., Davey, R. T., Youle, R. J. & Ackerman, E. J. Angiogenin is a cytotoxic, tRNA-specific ribonuclease in the RNase A superfamily. *J Biol Chem* **267**, 21982–21986 (1992).
35. Mazzanti, R. *et al.* Chronic viral hepatitis induced by hepatitis C but not hepatitis B virus infection correlates with increased liver angiogenesis. *Hepatology* **25**, 229–234 (1997).
36. Messerini, L., Novelli, L. & Comin, C. E. Microvessel density and clinicopathological characteristics in hepatitis C virus and hepatitis B virus related hepatocellular carcinoma. *J Clin Pathol* **57**, 867–871 (2004).
37. Walker, C. M. Comparative features of hepatitis C virus infection in humans and chimpanzees. *Springer Semin Immunopathol* **19**, 85–98 (1997).
38. Mason, W. S. *et al.* Detection of clonally expanded hepatocytes in chimpanzees with chronic hepatitis B virus infection. *J Virol* **83**, 8396–8408 (2009).
39. Jackman, J. E. & Alfonzo, J. D. Transfer RNA modifications: nature's combinatorial chemistry playground. *Wiley Interdisciplin Rev RNA* **4**, 35–48 (2013).

40. Kozomara, A. & Griffiths-Jones, S. miRBase: annotating high confidence microRNAs using deep sequencing data. *Nucleic Acids Res* **42**, D68–73 (2014).
41. Langmead, B., Trapnell, C., Pop, M. & Salzberg, S. L. Ultrafast and memory-efficient alignment of short DNA sequences to the human genome. *Genome Biol* **10**, R25 (2009).
42. David, M., Dzamba, M., Lister, D., Ilie, L. & Brudno, M. SHRiMP2: sensitive yet practical short read mapping. *Bioinformatics* **27**, 1011–2 (2011).
43. Larkin, M. A., Blackshields, G., Brown, N. P. & Chenna, R. Clustal W and Clustal X version 2.0. *Bioinformatics* **23**, 2947–2948 (2007).

Acknowledgments

This work was supported by grants from the National Institutes of Health: R00-DK091318 (P.S.); R01-AI095690 and R01-CA164029 (S.M.L); T32-GM067553 and T32-AI007419 (S.R.S). The Southwest National Primate Research Center is supported by a grant from the NIH Office of Research Infrastructure Programs/OD P51 OD011133), and by Research Facilities Improvement Program Grants C06 RR 12087 and C06 RR016228.

Author contributions

The experiments were designed by S.R.S., P.S. and S.M.L. The data were analyzed by S.R.S., J.B., T. Shirasaki, M.H., P.S. and S.M.L. Experiments were performed by S.R.S., D.Y., T.M., E.E.F., B.G. and T. Shirasaki. M.H., T. Shimakami, S.K., R.E.L., S.M.L. and P.S. contributed resources. The manuscript was written by S.R.S., P.S. and S.M.L.

Additional information

Supplementary information accompanies this paper at http://www.nature.com/scientificreports

Competing financial interests: The authors declare no competing financial interests.

How to cite this article: Selitsky, S.R. *et al.* Small tRNA-derived RNAs are increased and more abundant than microRNAs in chronic hepatitis B and C. *Sci. Rep.* **5**, 7675; DOI:10.1038/srep07675 (2015).

HEPATOLOGY
Official Journal of the American Association for the Study of Liver Diseases

Impaired Interferon Signaling in Chronic Hepatitis C Patients With Advanced Fibrosis via the Transforming Growth Factor Beta Signaling Pathway

Takayoshi Shirasaki,[1,2] Masao Honda,[1,2] Tetsuro Shimakami,[1] Kazuhisa Murai,[1,2] Takayuki Shiomoto,[1,2] Hikari Okada,[1] Riuta Takabatake,[1] Akihiro Tokumaru,[1] Yoshio Sakai,[1] Taro Yamashita,[1] Stanley M. Lemon,[3] Seishi Murakami,[1] and Shuichi Kaneko[1]

Malnutrition in the advanced fibrosis stage of chronic hepatitis C (CH-C) impairs interferon (IFN) signaling by inhibiting mammalian target of rapamycin complex 1 (mTORC1) signaling. However, the effect of profibrotic signaling on IFN signaling is not known. Here, the effect of transforming growth factor (TGF)-β signaling on IFN signaling and hepatitis C virus (HCV) replication was examined in Huh-7.5 cells by evaluating the expression of forkhead box O3A (Foxo3a), suppressor of cytokine signaling 3 (Socs3), c-Jun, activating transcription factor 2, ras homolog enriched in brain, and mTORC1. The findings were confirmed in liver tissue samples obtained from 91 patients who received pegylated-IFN and ribavirin combination therapy. TGF-β signaling was significantly up-regulated in the advanced fibrosis stage of CH-C. A significant positive correlation was observed between the expression of TGF-β2 and mothers against decapentaplegic homolog 2 (Smad2), Smad2 and Foxo3a, and Foxo3a and Socs3 in the liver of CH-C patients. In Huh-7.5 cells, TGF-β1 activated the Foxo3a promoter through an AP1 binding site; the transcription factor c-Jun was involved in this activation. Foxo3a activated the Socs3 promoter and increased HCV replication. TGF-β1 also inhibited mTORC1 and IFN signaling. Interestingly, c-Jun and TGF-β signaling was up-regulated in treatment-resistant IL28B minor genotype patients (TG/GG at rs8099917), especially in the early fibrosis stage. Branched chain amino acids or a TGF-β receptor inhibitor canceled these effects and showed an additive effect on the anti-HCV activity of direct-acting antiviral drugs (DAAs). *Conclusion:* Blocking TGF-β signaling could potentiate the antiviral efficacy of IFN- and/ or DAA-based treatment regimens and would be useful for the treatment of difficult-to-cure CH-C patients. (HEPATOLOGY 2014;60:1519-1530)

A human liver infected with hepatitis C virus (HCV) develops chronic hepatitis, cirrhosis, and in some instances, hepatocellular carcinoma (HCC). HCC develops frequently in the advanced fibrosis stage, and the annual incidence of HCC in patients with HCV-related liver cirrhosis is ~6-8%.[1] The eradication of HCV infection has been a promising prophylactic therapy for preventing the occurrence of HCC.

Interferon (IFN) and ribavirin (RBV) combination therapy has been a popular modality for eliminating HCV; however, its efficacy is limited in patients with advanced liver fibrosis.[2] The use of the recently developed direct-acting antiviral drugs (DAAs) telaprevir or

Abbreviations: AMPK, protein kinase, AMP-activated, alpha 1 catalytic subunit; CH-C, chronic hepatitis C; HCC, hepatocellular carcinoma; HCV, hepatitis C virus; IFN, interferon; IL28B, interleukin 28B; ISG-20, interferon-stimulated exonuclease gene 20; MX1, myxovirus resistance 1; NR, no response; RBV, ribavirin; RHEB, ras homolog enriched in brain; RIG-I, retinoic acid inducible gene I; SMAD, mothers against decapentaplegic homolog; TGF, transforming growth factor; TGF-RI, transforming growth factor-receptor inhibitor.

From the [1]Department of Gastroenterology, Kanazawa University Graduate School of Medicine, Kanazawa, Japan; [2]Department of Advanced Medical Technology, Kanazawa University Graduate School of Health Medicine, Kanazawa, Japan; [3]Division of Infectious Diseases, School of Medicine, University of North Carolina at Chapel Hill, Chapel Hill, NC, USA.

Received February 1, 2014; accepted June 20, 2014.

boceprevir, combined with pegylated (PEG)-IFN plus RBV, significantly improved the sustained virologic response (SVR) rates; however, the SVR rate is reduced in patients with advanced liver fibrosis and the treatment-resistant interleukin 28B (IL28B) genotype,[3-5] in whom HCC can develop at a high frequency. Moreover, extended therapy should be avoided in these patients in terms of the high frequency of adverse effects.

The mechanism of treatment resistance in patients with advanced liver fibrosis has not yet been clarified completely. Previously, we reported that the malnutrition status of patients with advanced chronic hepatitis C (CH-C) is associated with IFN resistance, and Fischer's ratio (branched chain amino acids [BCAAs] / aromatic amino acids) is an independent predictor of treatment outcome of PEG-IFN plus RBV combination therapy. Furthermore, we showed that malnutrition impaired IFN signaling by inhibiting mammalian target of rapamycin complex 1 (mTORC1) and activating suppressor of cytokine signaling 3 (Socs3)-mediated IFN inhibitory signaling through the nutrition-sensing transcriptional factor forkhead box protein O3a (Foxo3a).[6] This report represented the first clue to disentangling the molecular links between advanced CH-C and poor treatment response; however, the association of profibrotic signaling and IFN signaling was not evaluated in detail.

In the present study, we investigated the interaction between the signaling of the profibrotic gene transforming growth factor (TGF)-β and IFN signaling in the liver of CH-C patients. We showed that blocking TGF-β signaling as well as improving the nutritional status of patients by using BCAAs restored IFN signaling and increased the treatment efficacy of anti-HCV therapy.

Materials and Methods

Cell Lines. A reversibly immortalized human hepatocyte cell line (TTNT) was established by transduction with a retroviral vector containing cDNA expressing hTERT for immortalization.[7] TTNT, Huh-7, and Huh-7.5 cells (kindly provided by Professor C.M. Rice, Rockefeller University, New York, NY) were maintained in Dulbecco's modified Eagle's medium (DMEM; Gibco BRL, Gaithersburg, MD) containing 10% fetal bovine serum and 1% penicillin/streptomycin. Primary human hepatocytes (PHH) were isolated from chimeric mice with a humanized liver (PXB-mice; PhoenixBio, Hiroshima, Japan).

Amino Acid-Free Medium and BCAAs. Amino acid-free medium and BCAAs were prepared as described previously. Details are given in the Supporting Materials and Methods.

TGF-β and IFN Treatment. Huh-7.5 cells or HCV-RNA-transfected Huh-7.5 cells were seeded at 1.0×10^5 cells/well in 12-well plates. After 24 hours, the cells were treated with TGF-β (Millipore, Billerica, MA). At 24 hours later, the cells were treated with the indicated international units of IFN-α for 24 hours (Schering-Plough, Tokyo, Japan).

BCAA Treatment. HCV-RNA-transfected Huh-7.5 cells were seeded at 1.0×10^5 cells/well in 12-well plates. After 24 hours, the cells were treated with TGF-β in low-amino-acid medium and the indicated concentration of BCAAs. At 48 hours after treatment, real-time detection, polymerase chain reaction (RTD-PCR), western blotting, and *Gaussia* luciferase assays were carried out as described previously.

TGF-β Receptor Inhibitor Treatment. HCV-RNA-transfected Huh-7.5 cells were seeded at 1.0×10^5 cells/well in 12-well plates. After 24 hours, the cells were treated with TGF-β in low-amino-acid medium and TGF-β Receptor Inhibitor (TGF-β RI; Millipore). At 24 hours after treatment, RTD-PCR, western blotting, and *Gaussia* luciferase assays were carried out as described previously.

DAA Treatment. DAAs (boceprevir and BMS-790052) were purchased from AdooQ Bioscience (Irvine, CA). HCV-RNA-transfected Huh-7.5 cells were seeded at 1.0×10^5 cells/well in 12-well plates. After 24 hours, the cells were treated with TGF-β in low-amino-acid medium and BCAAs and DAAs. At 24 hours after treatment, the *Gaussia* luciferase assay was carried out as described previously.

Patients' characteristics, HCV replication analysis, western blotting, quantitative RTD-PCR, and promoter analysis are described in the Supporting Materials and Methods.

Address reprint requests to: Masao Honda, M.D., Ph.D., Department of Gastroenterology, Graduate School of Medicine, Kanazawa University, Takara-Machi 13-1, Kanazawa 920-8641, Japan. E-mail: mhonda@m-kanazawa.jp; fax: +81-76-234-4250.

View this article online at wileyonlinelibrary.com.

DOI 10.1002/hep.27277

Potential conflict of interest: Nothing to report.

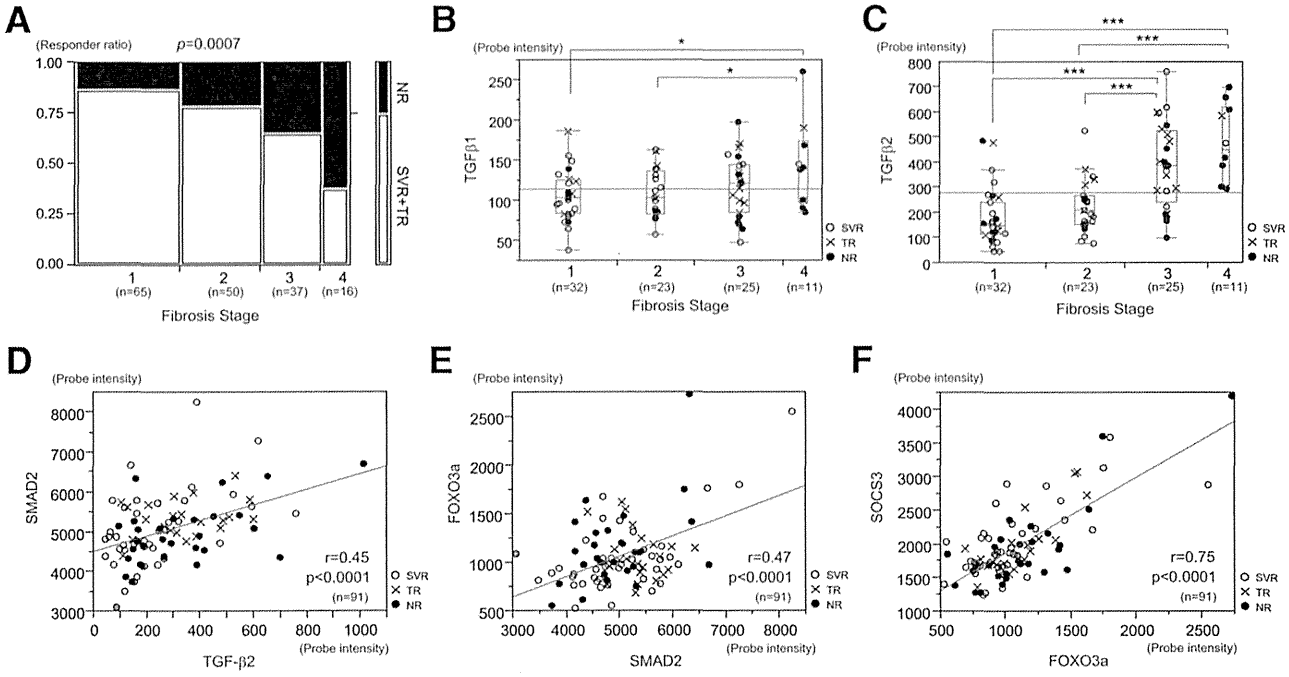

Fig. 1. Activation of TGF-β signaling in the liver of patients at the advanced fibrosis stage of CH-C. A: Significant increase in the NR ratio with the progression of fibrosis stage. B,C: Expression of TGF-β1 (B) and TGF-β2 (C) with the progression of fibrosis stage. D-F: Significant correlations of TGF-β2 and Smad2 (D), Smad2 and Foxo3a (E), and Foxo3a and Socs3 (F) expression in the liver of CH-C patients.

Statistical Analysis. The results are expressed as the mean value ± standard deviation. At least three samples were tested in each assay. Significance was tested by one-way analysis of variance with Bonferroni methods, and differences were considered statistically significant at $P < 0.05$.

Results

Up-Regulated TGF-β Signaling and Low Treatment Response in CH-C Patients With Advanced Liver Fibrosis Who Received PEG-IFN Plus RBV Combination Therapy. Previously, using a cohort of 168 CH-C patients who received PEG-IFN plus RBV combination therapy, we demonstrated that liver fibrosis stage and Fischer's ratio as well as IL28B genotype were independent significant factors associated with no response (NR) to treatment (Supporting Table 1).[6] The NR rate was significantly increased according to the increase in fibrosis stage ($P = 0.007$) (Fig. 1A). To reveal the molecular mechanism between profibrotic signaling and treatment resistance, we focused on TGF-β signaling in the liver of CH-C patients. The expression of TGF-β1 and TGF-β2, deduced from 91 CH-C patients whose liver tissues were analyzed previously using an Affymetrix GeneChip (Supporting Table 2),[6,8] was significantly up-regulated in the advanced fibrosis stage (Fig. 1B,C). In particular, the up-regulation of TGF-β2 in patients with stage 3 and 4 fibrotic livers was more prominent (Fig. 1C). There was a significant correlation between the expression of TGF-β2 and mothers against decapentaplegic homolog 2 (Smad2), a downstream signaling molecule of the TGF-β receptor, showing the activation of TGF-β signaling in the liver of CH-C patients. Interestingly, Smad2 expression was significantly correlated with Foxo3a expression, a nutrition-sensing transcription factor. Previously, we reported that Foxo3a increases the transcription of Socs3, an inhibitor of IFN signaling, through binding to the Socs3 promoter (Foxo3a-Socs3 signaling).[6] Foxo3a expression was significantly correlated with Socs3 expression in the CH-C patients (Fig. 1F).

TGF-β Signaling Activates Foxo3a-Socs3 Signaling in the Huh-7.5 Human Hepatoma Cell Line and PHH. The relationship between TGF-β and Foxo3a-Socs3 signaling was evaluated in PHH and the Huh-7.5 human hepatoma cell line without HCV replication (Huh-7.5 HCV (–)). This signaling was also evaluated in Huh-7.5 cells in which the infectious HCV clone H77Sv3 GLuc2A[6] was replicating (Huh-7.5 HCV (+)) (Fig. 2A). Treatment of these cells with TGF-β1 substantially increased the levels of phosphorylated (p)-Smad2 and p-Smad3. In this condition, the levels of p-Foxo3a, which is degraded through the proteasomal pathway,

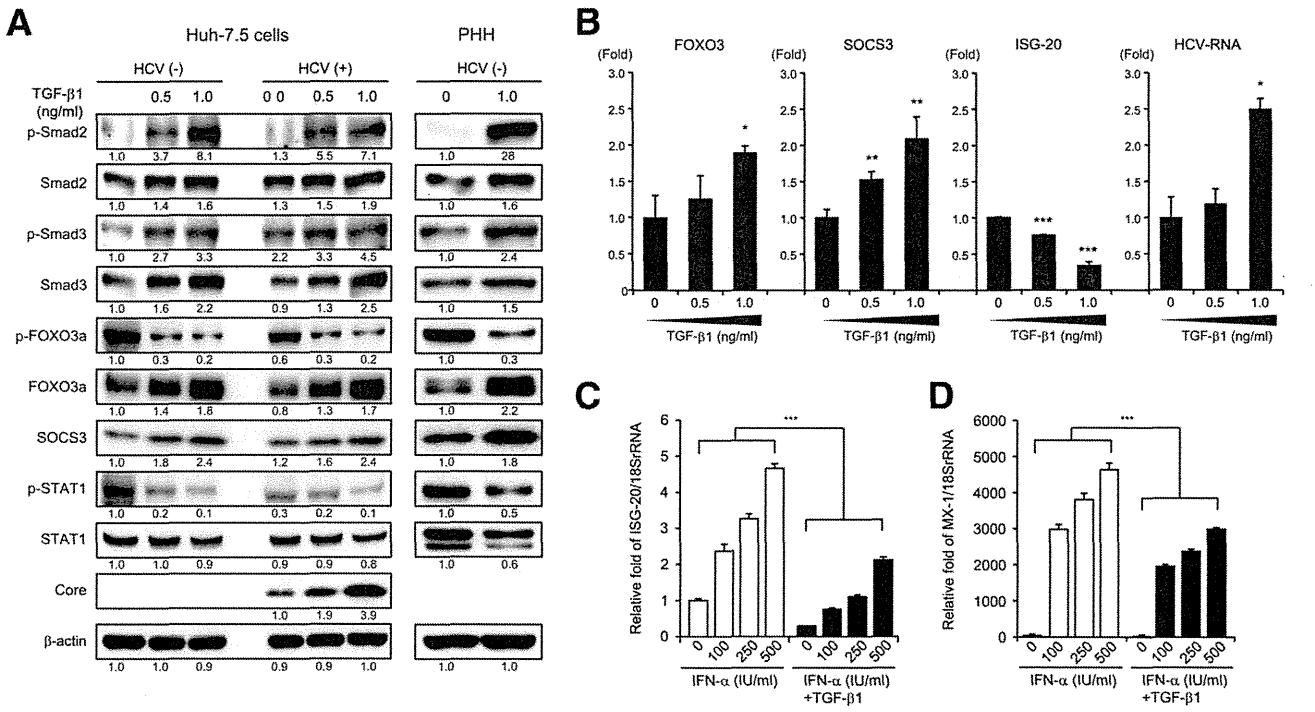

Fig. 2. Effect of TGF-β1 on IFN signaling in Huh-7.5 cells and PHH. A: Western blotting of TGF-β, Foxo3a-Socs3, and IFN signaling in Huh-7.5 cells and PHH treated with TGF-β1. Huh-7.5 cells were transfected with infectious HCV RNA, H77Sv3 GLuc2A prior to TGF-β1 treatment (Huh-7.5 HCV (+)). The experiments were repeated 3 times. B: RTD-PCR results for Foxo3a, Socs3, ISG-20, and HCV-RNA expression in Huh-7.5 HCV (+) treated with TGF-β1. C,D: Inhibition of IFN-α-induced ISG induction (ISG-20 [C] and MX1 [D]) by TGF-β1 in Huh-7.5 HCV (+). B-D: The experiments were performed in triplicate and repeated 3 times (*$P < 0.05$, **$P < 0.01$, ***$P < 0.001$).

decreased and total Foxo3a expression increased, and then Socs3 expression increased. Subsequently, the levels of phosphorylated signal transducer and activator of transcription 1 (p-STAT1) were decreased and the amount of HCV core protein increased in Huh-7.5 HCV (+). Thus, TGF-β signaling activated Foxo3a-Socs3 signaling and inhibited IFN signaling in hepatocytes, regardless of HCV replication and a loss-of-function mutation in retinoic acid inducible gene I (RIG-I).

These findings were also confirmed at the mRNA level in Huh-7.5 HCV (+). RTD-PCR showed that TGF-β1 treatment significantly increased Foxo3a and Socs3 expression, and decreased the expression of interferon-stimulated exonuclease gene 20 (ISG-20) in a dose-dependent manner. HCV-RNA was significantly increased in this condition (Fig. 2B). Moreover, the induction of interferon-stimulated genes (ISG-20 and myxovirus-resistance 1 [MX1]) by IFN-α treatment was significantly reduced in the presence of TGF-β1 (Fig. 2C,D).

When endogenous TGF-β signaling was compared between Huh-7.5 HCV (–) and Huh-7.5 HCV (+), TGF-β signaling was preactivated in Huh-7.5 HCV (+) before TGF-β1 treatment (Fig. 2A). To examine the role of endogenous TGF-β1 signaling on Foxo3a-Socs3 signaling and HCV replication, a small interfering (si) RNA specific to TGF-β1 was introduced to Huh-7 cells in which cell culture-derived infectious HCV HJ3-5 (HCVcc HJ3-5)[9] (Supporting Materials and Methods) was replicating. With the repression of TGF-β1, the levels of p-Smad2, p-Smad3, Foxo3a, and Socs3a decreased, while the levels of p-STAT1 increased. As a result, HCV replication deceased in both the amino acid-depleted (1/5 DMEM) and non-depleted (DMEM) conditions (Supporting Fig. 1).

AP1 Binding Site in the Foxo3a Promoter Is Responsible for the Induction of Foxo3a by TGF-β Signaling. To identify which transcription factors were involved in the induction of Foxo3a by TGF-β1, we cloned the upstream promoter region of Foxo3a and generated Foxo3a promoter-luciferase reporter constructs with various lengths of 5′-end deletions (−1780, −1340, and −801 nucleotides [nt]) (Fig. 3A). Luciferase activity deduced from pGL4-FOXO3a (−1780) increased by ~1.5-fold in the amino acid-depleted condition (1/5 DMEM) compared with the nondepleted condition (DMEM). TGF-β1 further stimulated the promoter activity of pGL4-FOXO3a (−1780) (Fig. 3B). A TGF-β1 RI canceled this stimulation (Fig. 3B). pGL4-FOXO3a (−1340) retained the regulation of promoter activity by amino acid depletion (1/5 DMEM) and

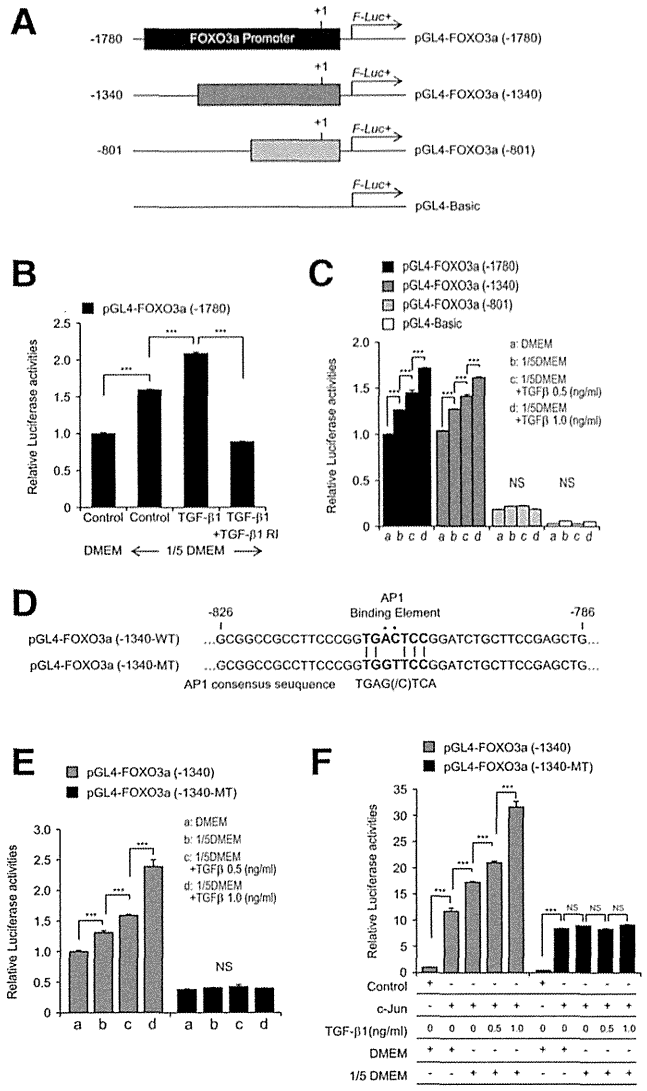

Fig. 3. Foxo3a promoter analysis. A: Foxo3a promoter-luciferase reporter constructs. B: Promoter activity of pGL4-FOXO3a (−1780) following amino acid depletion (1/5 DMEM), TGF-β1 treatment, and TGF-β1 RI treatment. C: Abolished regulation of the promoter activity of pGL4-FOXO3a (−801) by amino acid depletion (1/5 DMEM) and TGF-β1 treatment. D: Alignment of the AP1 binding element of pGL4-FOXO3a (−1340) and pGL4-FOXO3a (−1340-MT), in which the AP1 site was mutated. E: Abolished regulation of the promoter activity of pGL4-FOXO3a (−1340-MT) by amino acid depletion (1/5 DMEM) and TGF-β1 treatment. F: Overexpression of c-Jun, amino acid depletion (1/5 DMEM), and TGF-β1 treatment increased the promoter activity of pGL4-FOXO3a (−1340) by up to 32-fold, while these had less of an effect on the promoter activity of pGL4-FOXO3a (−1340-MT). The experiments were performed in triplicate and repeated 3 times ($*P < 0.05$, $**P < 0.01$, $***P < 0.001$).

TGF-β1 treatment; however, pGL4-FOXO3a (−801) lost this regulation (Fig. 3C), suggesting the presence of a response element between −1340 and −801 nt. We identified an activator protein (AP) 1 transcription factor binding site at −810 to −804 nt. (Fig. 3D). We introduced two nucleotide mutations (AC to GT) in the AP1 consensus binding sequence, and the mutant construct, pGL4-FOXO3a (−1340-MT), lost the response to amino acid depletion (1/5 DMEM) and TGF-β1 treatment (Fig. 3E). These results were confirmed by using three different hepatocyte-derived cell lines (TTNT, Huh-7, and Huh-7.5 cells; Supporting Fig. 2A-C). Although RIG-I-dependent IFN signaling was active in TTNT cells (Supporting Fig. 2D), Foxo3a promoter activity in response to amino acid depletion (1/5 DMEM) and TGF-β1 treatment was not significantly different between these cell lines.

To confirm these findings further, we overexpressed c-Jun, a component of AP1, and evaluated Foxo3a promoter activity. The overexpression of c-Jun increased the promoter activity of pGL4-FOXO3a (−1340) to 12-fold, and amino acid depletion (1/5 DMEM) and TGF-β1 treatment further increased promoter activity up to 32-fold (Fig. 3F). Conversely, pGL4-FOXO3a (−1340-MT) lost the response to amino acid depletion (1/5 DMEM) and TGF-β1 treatment (Fig. 3F). These results confirmed that AP1 plays an important role in the induction of Foxo3a by these stimulatory factors.

Transcription Factor c-Jun Is Involved in the Induction of Foxo3a in the Liver of CH-C Patients. The AP1 transcription factor is mainly composed of Jun, Fos, and activating transcription factor (ATF) protein dimers.[10] Therefore, we evaluated the expression of c-Jun, ATF2, and c-Fos in Huh-7.5 cells and PHH under amino acid depletion (1/5 DMEM) and TGF-β1 treatment. Western blotting analysis showed that the levels of p-c-Jun and p-ATF2 were increased under these conditions, although the induction of p-c-Jun by amino acid depletion (1/5 DMEM) was not obvious in PHH (Fig. 4A). These findings were also confirmed by RTD-PCR. The mRNA expression of c-Jun and ATF2 increased significantly, while the expression of c-Fos decreased (Supporting Fig. 3A-C). The overexpression of c-Jun in Huh-7.5 cells induced Foxo3a and Socs3 expression at the protein and mRNA levels (Supporting Fig. 3D,E). In the liver of CH-C patients, there were significant correlations between the expression of Smad2 and c-Jun, and c-Jun and Foxo3a (Fig. 4B,C). ATF2 expression was significantly correlated with c-Jun expression (Fig. 4D). Similarly, there were significant correlations between the expression of Smad2 and ATF2, and ATF2 and Foxo3a (Fig. 4E,F). These results suggested that c-Jun and possibly ATF2, but not c-Fos, might be involved in TGF-β-Foxo3a signaling.

TGF-β Signaling Induces Socs3 Through the Induction of Foxo3a. Previously, we reported that Foxo3a increases the transcription of Socs3 through its binding to the Socs3 promoter region.[6] We confirmed

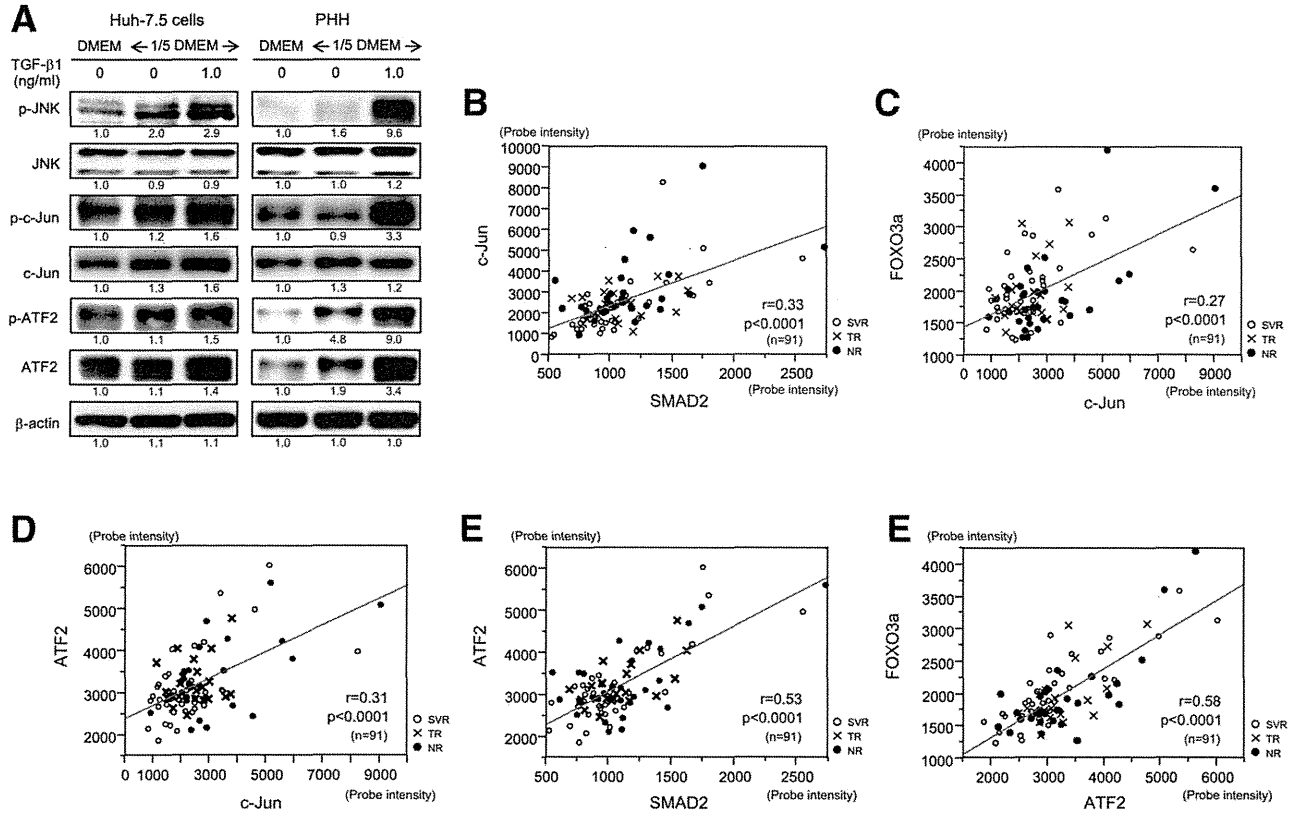

Fig. 4. TGF-β signaling up-regulates the expression of the transcription factors c-Jun and ATF2 in Huh-7.5 cells, PHH, and the liver of CH-C patients. A: Western blotting of JNK, c-Jun, and ATF2 in Huh-7.5 cells and PHH treated with amino acid depletion (1/5 DMEM) and TGF-β1. The experiments were repeated 3 times. B-F: Significant correlations of Smad2 and c-Jun (B), Foxo3a and c-Jun (C), c-Jun and ATF2 (D), Smad2 and ATF2 (E), and ATF2 and Foxo3a (F) expression in the liver of CH-C patients.

these findings in more detail in conjunction with TGF-β signaling. The overexpression of Foxo3a increased Socs3 expression in the nonamino acid-depleted condition (DMEM), and Socs3 was further induced in the amino acid-depleted condition (1/5 DMEM) and by TGF-β1 treatment (Supporting Fig. 4A). HCV-RNA was similarly increased in these conditions (Supporting Fig. 4B). Foxo3a mRNA expression, as deduced from RTD-PCR, was increased up to 7-fold in the combination of amino acid depletion (1/5 DMEM), c-Jun overexpression, and TGF-β1 treatment (Supporting Fig. 4C). Socs3 mRNA expression was up-regulated by 8-fold in the same conditions (Supporting Fig. 4D). The promoter activity of Socs3 was significantly increased by amino acid depletion (1/5 DMEM) and TGF-β1 treatment (pGL4-SOCS3-WT, Supporting Fig. 4E), while mutation of the Foxo3a binding site in the Socs3 promoter (pGL4-SOCS3-MT) abrogated this regulation. These results confirmed that TGF-β signaling up-regulated the expression of Socs3 through the induction of Foxo3a.

TGF-β Signaling Suppresses mTORC1 Signaling. Previously, we demonstrated that malnutrition decreased mTORC1 and IFN signaling using Huh-7 cells and clinical samples.[6] In the present study, we examined the effect of TGF-β signaling on mTORC1 signaling. In Huh-7.5 cells and PHH, amino acid depletion (1/5 DMEM) repressed mTORC1 signaling, as demonstrated by the decreased expression of ras homolog enriched in brain (RHEB),[11] a stimulator of mTORC1 signaling, p-mTOR, and p-p70S6K (Fig. 5A). Interestingly, TGF-β1 further decreased this expression. The decreased mTORC1 signaling was independent of AMP-activated, alpha 1 catalytic subunit (AMPK), a suppressor of mTORC1 signaling, as the levels of p-AMPK were rather decreased by amino acid depletion (1/5 DMEM) and TGF-β1 treatment in Huh-7.5 cells and PHH (Fig. 5A). It could be speculated that TGF-β signaling, combined with malnutrition, repressed the expression of RHEB and induced the expression of Foxo3a, which leads to the impaired IFN signaling observed in the advanced fibrosis stage of CH-C (Fig. 5B). In the liver of CH-C

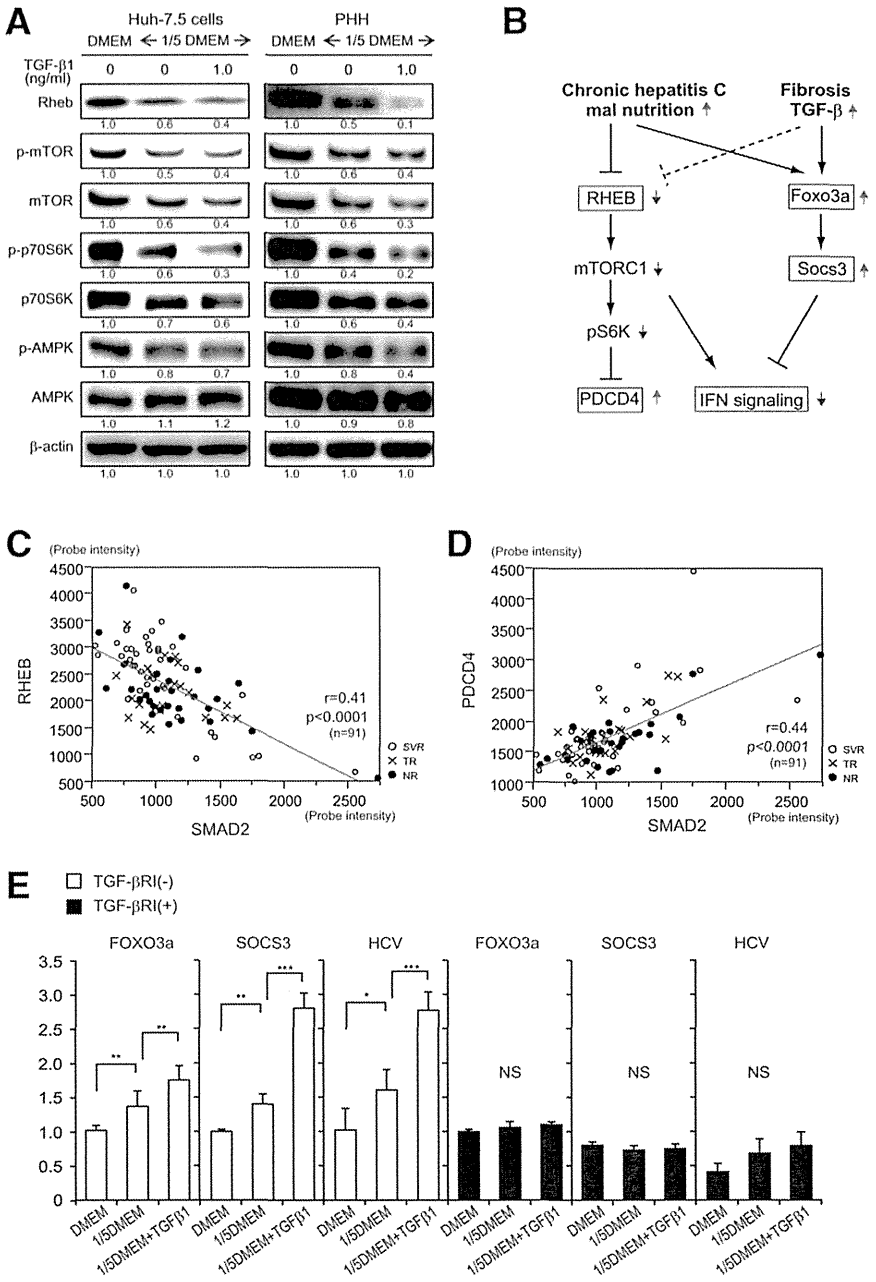

Fig. 5. TGF-β signaling represses mTORC1 signaling in Huh-7.5 cells, PHH, and the liver of CH-C patients. A: Western blotting of RHEB, mTOR, p70S8K, and AMPK in Huh-7.5 cells and PHH treated with amino acid depletion (1/5 DMEM) and TGF-β1. The experiments were repeated 3 times. B: Schematic representation of the effects of malnutrition and TGF-β signaling on IFN signaling. C,D: Significant correlations of Smad2 and RHEB (C), and Smad2 and PDCD4 (D) expression in the liver of CH-C patients. E: Blocking TGF-β signaling by TGF-β1 RI treatment abolishes the increase in Foxo3a, Socs3, and HCV replication by amino acid depletion (1/5 DMEM) and TGF-β1 treatment. The experiments were performed in triplicate and repeated 3 times ($^*P < 0.05$, $^{**}P < 0.01$, $^{***}P < 0.001$).

patients, Smad2 expression was significantly negatively correlated with RHEB expression. The expression of programmed cell death 4 (PDCD4), which is negatively regulated by mTORC1 signaling at the transcriptional level (Fig. 5C),[12] was significantly positively correlated with Smad2 expression (Fig. 5D).

We further examined the effect of TGF-β1 on IFN signaling by using TGF-β RI. TGF-β RI substantially repressed the levels of p-Smad2 and p-Smad3 (Supporting Fig. 5). TGF-β RI abolished the induction of Foxo3a expression and the subsequent induction of Socs3 by amino acid depletion (1/5 DMEM) and TGF-β1 treatment (Fig. 5E). HCV replication in normal medium (DMEM), as deduced from *Gaussia* luciferase activity, was repressed by TGF-β RI, and the increase in HCV replication by amino acid depletion (1/5 DMEM) and TGF-β1 treatment was abrogated (Fig. 5E).

c-Jun Is Up-Regulated in the Liver of NR and Treatment-Resistant IL28B Minor Genotype Patients. We evaluated the clinical significance of c-Jun for treatment response. The expression of c-Jun was significantly higher in NR patients than in responder patients (SVR+TR) (Fig. 6A). Furthermore, c-Jun expression was significantly higher in patients with the treatment-resistant IL28B minor genotype

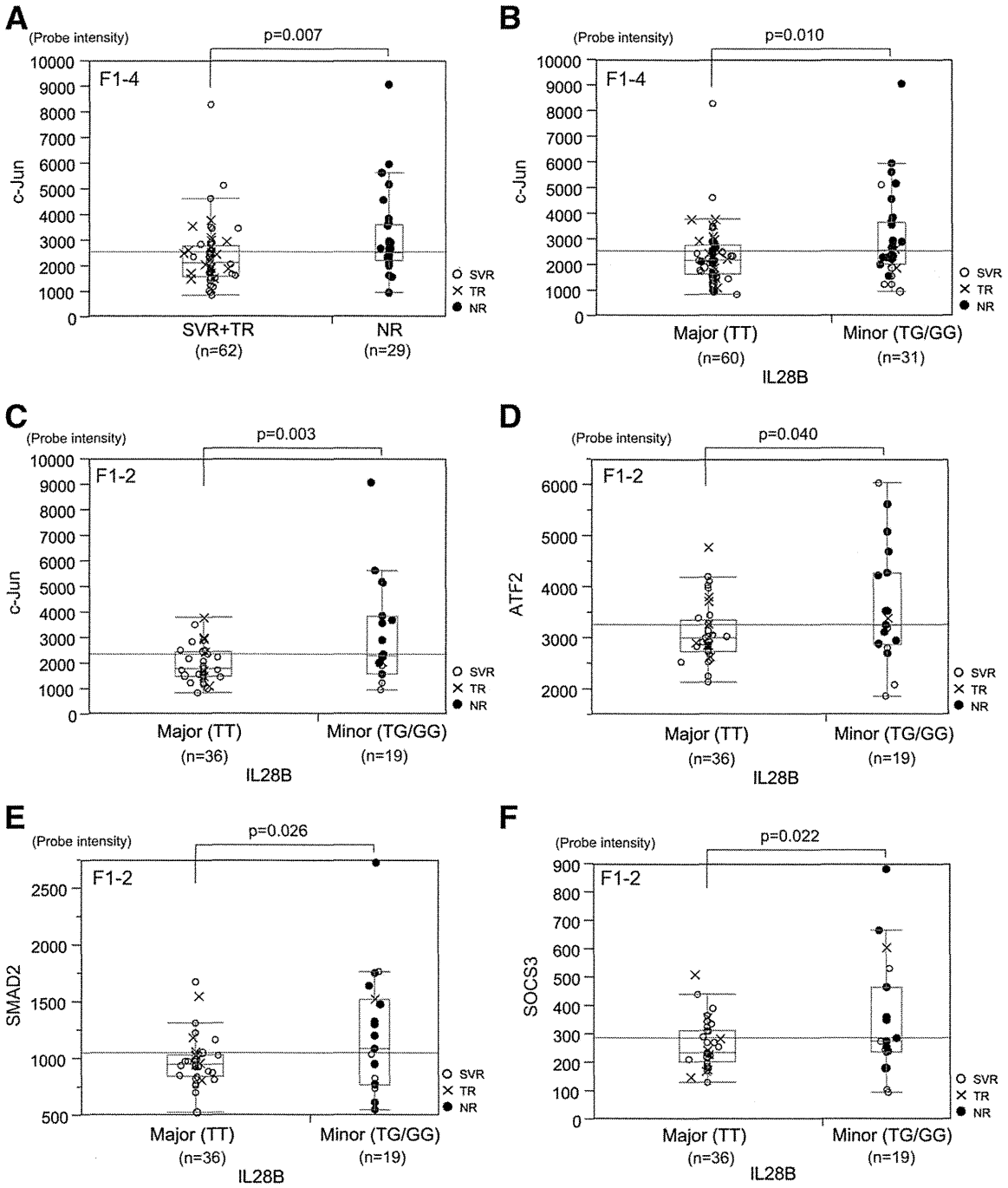

Fig. 6. Relationship between TGF-β signaling and treatment response and the IL28B genotype. The expression of c-Jun was up-regulated in NR (A) and IL28B minor genotype (TG/GG at rs8099917) (B) patients in all fibrosis stages (F1-4). The expression of ATF2 (D), Smad2 (E), and Socs3 (F) was up-regulated in IL28B minor genotype (TG/GG at rs8099917) patients at early fibrosis stages (F1-2).

(TG/GG at rs8099917) than in those with the treatment-sensitive IL28B major genotype (TT) (Fig. 6B).[5] Interestingly, TGF-β signaling was more activated in patients with the treatment-resistant IL28B minor genotype at an early stage of liver fibrosis (F1 and F2). The expression of c-Jun, ATF2, Smad2, and Socs3 was significantly higher in IL28B minor genotype patients (Fig. 6C-F).

BCAAs Inhibit TGF-β Signaling and Restore IFN Signaling. Previously, we reported that BCAAs restored IFN signaling in the amino acid-depleted condition (1/5 DMEM) by activating mTORC1 signaling and suppressing Foxo3a-Socs3 signaling.[6] In the present study, we examined whether BCAAs could inhibit TGF-β signaling and restore IFN signaling. Western

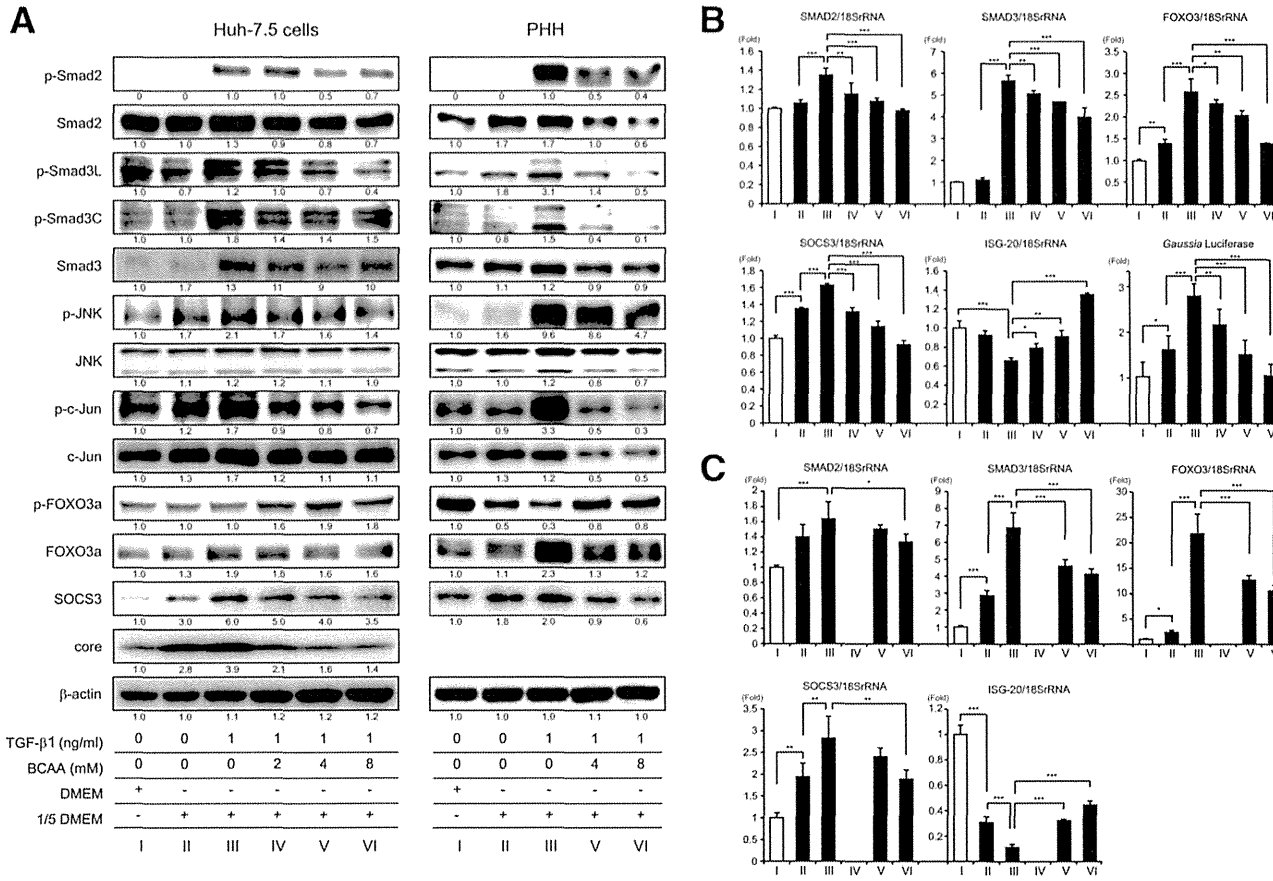

Fig. 7. BCAAs inhibit the effect of malnutrition and TGF-β signaling in Huh-7.5 cells and PHH. A: Western blotting of TGF-β and Foxo3a-Socs3 signaling in Huh-7.5 HCV (+) and PHH treated with amino acid depletion (1/5 DMEM), TGF-β1, and BCAAs. B,C: mRNA expression of TGF-β, Foxo3a-Socs3, and IFN signaling in Huh-7.5 HCV (+) (B) and PHH (C) treated with amino acid depletion (1/5 DMEM), TGF-β1, and BCAA.

blotting analysis showed that BCAAs dose-dependently repressed the expression of p-Smad3L, p-Smad3C, p-JNK, p-c-Jun, Foxo3a, Socs3 (in Huh-7.5 cells and PHH), and HCV core protein (in Huh-7.5 cells), which was induced by amino acid depletion (1/5 DMEM) and TGF-β1 treatment (Fig. 7A). RTD-PCR demonstrated similar mRNA expression patterns (Smad2, Smad3, Foxo3a, and Socs3a) to those obtained by western blotting (Fig. 7B,C), and BCAAs induced the expression of ISG-20 (in Huh-7.5 cells and PHH) and decreased HCV replication in a dose-dependent manner (in Huh-7.5 cells) (Fig. 7B). These results were also confirmed in HCVcc HJ3-5-infected Huh-7 cells (Supporting Fig. 6).

BCAAs and TGF-β RI Potentiate the Anti-HCV Activity of DAAs. Finally, we examined whether BCAAs or TGF-β RI potentiate the anti-HCV activity of DAAs. Amino acid depletion (1/5 DMEM) and TGF-β1 treatment significantly increased HCV replication (deduced from *Gaussia* luciferase activity), and BCAAs (8 mM) and boceprevir (250 nM; NS3 protease inhibitor) inhibited HCV replication to 64% and 50%, respectively (Fig. 8A, black bars). The combination of BCAAs (8 mM) and boceprevir (250 nM) further inhibited HCV replication to 10% and canceled the effect of amino acid depletion (1/5 DMEM) and TGF-β1 treatment, which supported HCV replication (Fig. 8A, compare white and black bars). Similarly, TGF-β RI (10 μM) repressed HCV replication to 60%, and its combination with boceprevir (250 nM) decreased HCV replication to 16% (Fig. 8B, black bars) and canceled the effect of amino acid depletion (1/5 DMEM) and TGF-β1 treatment (Fig. 8A, compare white and black bars). Thus, BCAAs and TGF-β RI had an additive effect on the anti-HCV activity of boceprevir and would be useful for CH-C patients with advanced fibrosis and the IL28B treatment-resistant genotype. A similar effect was obtained by using the NS5A inhibitor BMS-790052; however, its effect was less than that of boceprevir (Supporting Fig. 7).

Discussion

The recently developed DAAs have significantly improved the efficacy of anti-HCV therapy. Triple

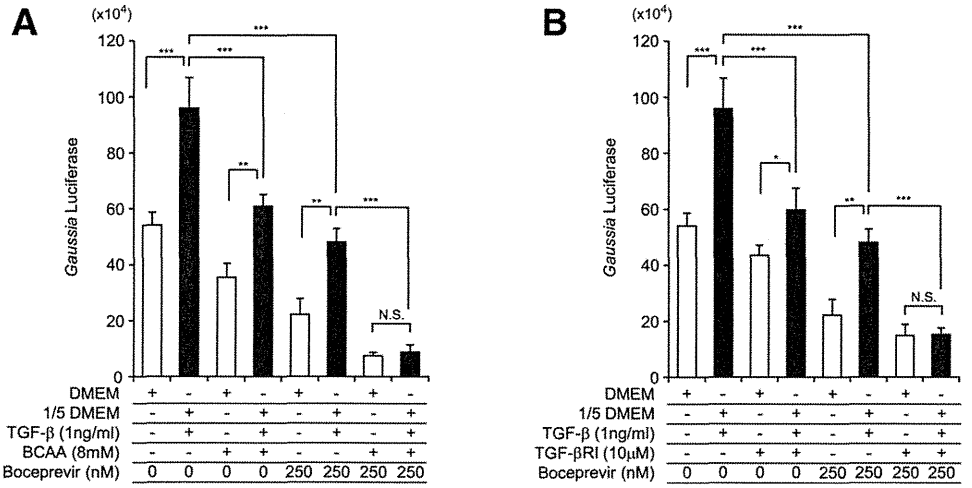

Fig. 8. Anti-HCV activity of boceprevir in combination with BCAAs (A) and TGF-β1 RI (B). HCV replication in Huh-7.5 cells was deduced by *Gaussia* luciferase activity. Boceprevir in combination with BCAAs (A) and TGF-β1 RI (B) efficiently repressed HCV replication in Huh-7.5 cells treated with amino acid depletion (1/5 DMEM) and TGF-β1. The experiments were performed in triplicate and repeated 3 times ($*P < 0.05$, $**P < 0.01$, $***P < 0.001$).

therapy comprising PEG-IFN, RBV, and DAA (e.g., telaprevir or boceprevir) has significantly increased SVR rates; however, its efficacy is poor in difficult-to-cure patients such as those with cirrhosis and the IL28B treatment-resistant genotype.[2,4] An IFN-free regimen using a combination of DAAs would be effective to treat these difficult-to-cure patients; however, the emergence of multiple drug resistant viruses and the high cost of these therapies should be considered carefully in the future. Therefore, standard PEG-IFN plus RBV combination therapy is still useful as an alternative therapy for CH-C.

Previously, we reported that malnutrition in patients with the advanced fibrosis stage of CH-C is associated with IFN resistance and impaired IFN signaling by inhibiting mTORC1 and activating Socs3-mediated IFN inhibitory signaling through the nutrition-sensing transcriptional factor Foxo3a.[6] However, the effect of profibrosis signaling on IFN signaling was not addressed in our previous study. In the present study, using clinical samples and cell lines, we clearly showed that TGF-β signaling inhibits IFN signaling by activating Foxo3a-Socs3-mediated IFN inhibitory signaling (Figs. (1 and 4)) and inhibiting mTORC1 signaling (Fig. 5).

Using Foxo3a promoter-luciferase reporter constructs, we showed that TGF-β1 activated Foxo3a promoter activity through an AP1 transcription factor binding site. Among the components of AP1, c-Jun and probably ATF2, but not c-Fos, were involved in this induction. Previous reports showed that c-Jun and ATF2 were induced by amino acid depletion[13,14] and TGF-β1 treatment,[15,16] although the induction of c-Jun by amino acid depletion was not obvious in PHH in this study. It could be considered that malnutrition and profibrotic signaling cooperatively activated the Foxo3a promoter through the AP1 site and that c-Jun induction was more specifically regulated by TGF-β1 in normal hepatocytes. Mutation of the AP1 binding site (pGL4-FOXO3a [-1340-MT]) abolished the response to amino acid depletion (1/5 DMEM) and TGF-β1 treatment (Fig. 3E; Supporting Fig. 2). Conversely, c-Jun overexpression combined with amino acid depletion (1/5 DMEM) and TGF-β1 treatment activated the Foxo3a promoter by 32-fold (Fig. 3F). In addition, we showed that TGF-β1 inhibited mTORC1 signaling, as demonstrated by the decreased expression of RHEB, p-mTOR, and p-p70S6K (Fig. 5A).

These results were in concordance with gene expression in the liver of CH-C patients. The expression of c-Jun and ATF2 was significantly correlated with Smad2 and Foxo3a expression, respectively (Fig. 4), while the expression of RHEB was significantly negatively correlated with Smad2 expression in the liver of CH-C patients (Fig. 5C). In this study, TGF-β1 and TGF-β2 expression was up-regulated in advanced liver fibrosis, and the expression of TGF-β2 was well correlated with the downstream signaling molecule Smad2 (Fig. 1B-D). Although we could not address the biological differences in TGF-β isoforms in this study, TGF-β1 and TGF-β2 reportedly mediate a similar signaling pathway to induce profibrotic responses.[17] Collectively, TGF-β signaling inhibited IFN signaling by activating Foxo3a-Socs3 IFN inhibitory signaling and

inhibiting mTORC1-IFN stimulating signaling *in vitro* and *in vivo*. Recently, Lee et al. showed that Foxo3a regulates the TGF-β1 promoter directly.[18] Combining their data and ours, there must be positive feedback regulation between TGF-β1 and Foxo3a. Moreover, they identified a polymorphism in Foxo3a (rs12212067: T > G) in which the minor (G) allele was involved in the increased production of TGF-β1 and associated with the inflammatory response.[18] We genotyped the Foxo3a rs12212067 polymorphism in three cell lines and observed TT in Huh-7 and Huh-7.5 and GG in TTNT (Supporting Table 3). Although we could not find a significant difference in Foxo3a promoter activity in response to TGF-β1 among these cell lines (Supporting Fig. 2), further studies should be performed to compare Foxo3a-Socs3 IFN inhibitory signaling among them. Furthermore, it is worthwhile to examine the relationship between the genotype at rs12212067 and treatment response and severity of liver disease in CH-C patients in the future.

Another interesting finding in this study was that TGF-β signaling was related to the IL28B genotype (Fig. 6). The expression of c-Jun was significantly higher in IL28B treatment-resistant minor genotype (TG/GG at rs8099917) patients than in IL28B treatment-sensitive major genotype (TT) patients. Moreover, the expression of c-Jun, Smad2, ATF2, and Socs3 was up-regulated more in IL28B minor genotype patients than in IL28B major genotype patients, especially in those with early stage liver fibrosis (F1-2). The underlying mechanisms of these findings are not known so far; however, we recently reported that the noncanonical WNT signaling ligand WNT5A is up-regulated in the liver of IL28B minor genotype patients and plays a role in treatment resistance.[19] WNT5A reportedly mediates downstream signaling through c-Jun and ATF2 in *Xenopus* cells and human osteosarcoma cells.[20,21] It could be speculated that WNT5A potentiates TGF-β signaling through these transcription factors, although this hypothesis should be tested in the future.

We examined whether BCAAs and TGF-β RI improve the IFN inhibitory signaling induced by malnutrition and TGF-β signaling (Fig. 7). Previously, we demonstrated that BCAAs improved the IFN signaling that was inhibited by malnutrition.[6] In the present study, we found that BCAAs blocked TGF-β signaling by decreasing the levels of p-Smad3L, p-JNK, and c-Jun (Fig. 7A). Consequently, BCAAs decreased the expression of Foxo3a, Socs3, and HCV core protein (Fig. 7). In addition, we found that the combination of BCAAs or TGF-β RI and the NS3 protease inhibitor boceprevir efficiently inhibited HCV replication and canceled the positive effects of malnutrition and TGF-β1 on HCV replication (Fig. 8). A recent report showed that the NS3 protease of HCV mimics TGF-β2 and activates the TGF-β type I receptor.[22] Therefore, the anti-HCV effect of boceprevir could be potentiated in combination with BCAAs or TGF-β RI, which blocked TGF-β signaling and increased IFN signaling. Therefore, the combination of BCAAs or TGF-β RI with DAAs could be useful for the treatment of difficult-to-cure CH-C patients with advanced liver fibrosis and the IL28B treatment-resistant genotype.

In conclusion, we clarified that TGF-β signaling inhibits IFN signaling and is related to the treatment-resistant phenotype of CH-C patients with advanced liver fibrosis and the IL28B treatment-resistant genotype. Furthermore, blocking TGF-β signaling by BCAAs or TGF-β RI could potentiate the anti-HCV effect of DAAs. An oral TGF-β RI small compound, LY2157299, is now being assessed in a phase II trial for the treatment of advanced-stage HCC. Further studies should be performed to address the significance of these compounds for the eradication of HCV in patients with advanced liver fibrosis for preventing HCC.

Acknowledgment: The authors thank Mina Nishiyama for technical assistance.

Author Contributions: Takayoshi Shirasaki performed most experiments and drafted the article; Masao Honda, study design, interpretation of data, and drafting of the article; Tetsuro Shimakami, HCV replication analysis and cellular experiments; Kazuhisa Murai, HCV replication analysis and cellular experiments; Takayuki Shiomoto, HCV replication analysis and cellular experiments; Hikari Okada, HCV replication analysis and cellular experiments; Riuta Takabatake, HCV replication analysis and cellular experiments; Akihiro Tokumaru, HCV replication analysis and cellular experiments; Yoshio Sakai, acquisition of clinical data; Taro Yamashita, acquisition of clinical data; Stanley M. Lemon, study design and interpretation of data; Seishi Murakami, study design and interpretation of data; Shuichi Kaneko, study concept and design.

References

1. Yoshida H, Shiratori Y, Moriyama M, Arakawa Y, Ide T, Sata M, et al. Interferon therapy reduces the risk for hepatocellular carcinoma: national surveillance program of cirrhotic and noncirrhotic patients with chronic hepatitis C in Japan IHIT Study Group. Inhibition of Hepatocarcinogenesis by Interferon Therapy. Ann Intern Med 1999;131:174-181.

2. Trembling PM, Tanwar S, Rosenberg WM, Dusheiko GM. Treatment decisions and contemporary versus pending treatments for hepatitis C. Nat Rev Gastroenterol Hepatol 2013;10:713-728.
3. Hezode C, Fontaine H, Dorival C, Larrey D, Zoulim F, Canva V, et al. Triple therapy in treatment-experienced patients with HCV-cirrhosis in a multicentre cohort of the French Early Access Programme (ANRS CO20-CUPIC) – NCT01514890. J Hepatol 2013;59:434-441.
4. Bruno S, Vierling JM, Esteban R, Nyberg LM, Tanno H, Goodman Z, et al. Efficacy and safety of boceprevir plus peginterferon-ribavirin in patients with HCV G1 infection and advanced fibrosis/cirrhosis. J Hepatol 2013;58:479-487.
5. Tanaka Y, Nishida N, Sugiyama M, Kurosaki M, Matsuura K, Sakamoto N, et al. Genome-wide association of IL28B with response to pegylated interferon-alpha and ribavirin therapy for chronic hepatitis C. Nat Genet 2009;41:1105-1109.
6. Honda M, Takehana K, Sakai A, Tagata Y, Shirasaki T, Nishitani S, et al. Malnutrition impairs interferon signaling through mTOR and FoxO pathways in patients with chronic hepatitis C. Gastroenterology 2011;141:128-140.
7. Okitsu T, Kobayashi N, Jun HS, Shin S, Kim SJ, Han J, et al. Transplantation of reversibly immortalized insulin-secreting human hepatocytes controls diabetes in pancreatectomized pigs. Diabetes 2004;53:105-112.
8. Honda M, Nakamura M, Tateno M, Sakai A, Shimakami T, Shirasaki T, et al. Differential interferon signaling in liver lobule and portal area cells under treatment for chronic hepatitis C. J Hepatol 2010;53:817-826.
9. Yi M, Ma Y, Yates J, Lemon SM. Compensatory mutations in E1, p7, NS2, and NS3 enhance yields of cell culture-infectious intergenotypic chimeric hepatitis C virus. J Virol 2007;81:629-638.
10. Eferl R, Wagner EF. AP-1: a double-edged sword in tumorigenesis. Nat Rev Cancer 2003;3:859-868.
11. Bai X, Ma D, Liu A, Shen X, Wang QJ, Liu Y, et al. Rheb activates mTOR by antagonizing its endogenous inhibitor, FKBP38. Science 2007;318:977-980.
12. Carayol N, Katsoulidis E, Sassano A, Altman JK, Druker BJ, Platanias LC. Suppression of programmed cell death 4 (PDCD4) protein expression by BCR-ABL-regulated engagement of the mTOR/p70 S6 kinase pathway. J Biol Chem 2008;283:8601-8610.
13. Chaveroux C, Jousse C, Cherasse Y, Maurin AC, Parry L, Carraro V, et al. Identification of a novel amino acid response pathway triggering ATF2 phosphorylation in mammals. Mol Cell Biol 2009;29:6515-6526.
14. Fu L, Balasubramanian M, Shan J, Dudenhausen EE, Kilberg MS. Auto-activation of c-JUN gene by amino acid deprivation of hepatocellular carcinoma cells reveals a novel c-JUN-mediated signaling pathway. J Biol Chem 2011;286:36724-36738.
15. Sano Y, Harada J, Tashiro S, Gotoh-Mandeville R, Maekawa T, Ishii S. ATF-2 is a common nuclear target of Smad and TAK1 pathways in transforming growth factor-beta signaling. J Biol Chem 1999;274:8949-8957.
16. Mu Y, Gudey SK, Landstrom M. Non-Smad signaling pathways. Cell Tissue Res 2012;347:11-20.
17. Leask A, Abraham DJ. TGF-beta signaling and the fibrotic response. FASEB J 2004;18:816-827.
18. Lee JC, Espeli M, Anderson CA, Linterman MA, Pocock JM, Williams NJ, et al. Human SNP links differential outcomes in inflammatory and infectious disease to a FOXO3-regulated pathway. Cell 2013;155:57-69.
19. Honda M, Shirasaki T, Shimakami T, Sakai A, Horii R, Arai K, et al. Hepatic interferon-stimulated genes are differentially regulated in the liver of chronic hepatitis C patients with different interleukin 28B genotypes. HEPATOLOGY 2014;59:828-838.
20. Yamanaka H, Moriguchi T, Masuyama N, Kusakabe M, Hanafusa H, Takada R, et al. JNK functions in the non-canonical Wnt pathway to regulate convergent extension movements in vertebrates. EMBO Rep 2002;3:69-75.
21. Yamagata K, Li X, Ikegaki S, Oneyama C, Okada M, Nishita M, et al. Dissection of Wnt5a-Ror2 signaling leading to matrix metalloproteinase (MMP-13) expression. J Biol Chem 2012;287:1588-1599.
22. Sakata K, Hara M, Terada T, Watanabe N, Takaya D, Yaguchi S, et al. HCV NS3 protease enhances liver fibrosis via binding to and activating TGF-beta type I receptor. Sci Rep 2013;3:3243.

Supporting Information

Additional Supporting Information may be found in the online version of this article at the publisher's website.

nature medicine

Regulation of the hepatitis C virus RNA replicase by endogenous lipid peroxidation

Daisuke Yamane[1,2], David R McGivern[1,2], Eliane Wauthier[2,3], MinKyung Yi[4], Victoria J Madden[5], Christoph Welsch[6], Iris Antes[7], Yahong Wen[8], Pauline E Chugh[2,9], Charles E McGee[10], Douglas G Widman[11], Ichiro Misumi[10], Sibali Bandyopadhyay[12,13], Seungtaek Kim[1,2,14], Tetsuro Shimakami[1,2], Tsunekazu Oikawa[2,3], Jason K Whitmire[2,9,10], Mark T Heise[2,10], Dirk P Dittmer[2,9], C Cheng Kao[8], Stuart M Pitson[15], Alfred H Merrill Jr[12,13], Lola M Reid[2,3] & Stanley M Lemon[1,2,9]

Oxidative tissue injury often accompanies viral infection, yet there is little understanding of how it influences virus replication. We show that multiple hepatitis C virus (HCV) genotypes are exquisitely sensitive to oxidative membrane damage, a property distinguishing them from other pathogenic RNA viruses. Lipid peroxidation, regulated in part through sphingosine kinase-2, severely restricts HCV replication in Huh-7 cells and primary human hepatoblasts. Endogenous oxidative membrane damage lowers the 50% effective concentration of direct-acting antivirals *in vitro*, suggesting critical regulation of the conformation of the NS3-4A protease and the NS5B polymerase, membrane-bound HCV replicase components. Resistance to lipid peroxidation maps genetically to transmembrane and membrane-proximal residues within these proteins and is essential for robust replication in cell culture, as exemplified by the atypical JFH1 strain of HCV. Thus, the typical, wild-type HCV replicase is uniquely regulated by lipid peroxidation, providing a mechanism for attenuating replication in stressed tissue and possibly facilitating long-term viral persistence.

Reactive oxygen species (ROS) are an unavoidable byproduct of aerobic metabolism and a double-edged sword for complex cellular systems[1]. Although central to many disease states, ROS also function as second messengers during embryonic development and, in macrophages, contribute to host defense against infection[2,3]. Viral infections frequently induce ROS generation, either by stimulating host immune responses or by direct tissue injury[4]. HCV, a hepatotropic RNA virus with a unique capacity for persistence[5], induces substantial intrahepatic oxidative stress, thereby promoting liver injury[6,7]. Limited data suggest that lipid peroxidation restricts HCV replication[8], but how it impairs the viral replicative machinery is unknown.

Although HCV is a leading cause of cirrhosis and liver cancer[5], many details of its replication remain obscure, as most HCV strains replicate poorly in cell culture. A notable exception is JFH1, a genotype 2a virus recovered from a patient with fulminant hepatitis[9]. JFH1 recapitulates the entire virus life cycle and replicates efficiently in Huh-7 hepatoma cells[9–11]. In recent years, it has become a laboratory standard used in most studies of HCV replication. However, there is very limited understanding of the robust replication phenotype that sets it apart from other HCVs[12,13].

Like all positive-strand RNA virus genomes, the HCV genome is synthesized by a multiprotein replicase complex that assembles in association with intracellular membranes. Known as the 'membranous web' in HCV-infected cells[14,15], this specialized cytoplasmic compartment provides a platform for viral RNA synthesis. Its membranes are enriched in cholesterol, sphingolipids and phosphatidylinositol-4-phosphate[16,17]. Assembly of the membranous web involves recruitment of phosphatidylinositol-4-phosphate-3 kinase and annexin A2 (refs. 17–19) and possibly also direct membrane remodeling by nonstructural HCV proteins[20]. Whereas lipid metabolism also plays key roles in later steps in the virus life cycle[21], these modifications of intracellular membranes are closely linked to viral RNA synthesis.

Sphingolipids are increased in abundance within the replicase membranes and are important factors in HCV replication[22–25]. Sphingomyelin interacts with and in some genotypes stimulates NS5B, the viral RNA-dependent RNA polymerase[23,26]. While studying

[1]Department of Medicine, Division of Infectious Diseases, The University of North Carolina at Chapel Hill, Chapel Hill, North Carolina, USA. [2]Lineberger Comprehensive Cancer Center, The University of North Carolina at Chapel Hill, Chapel Hill, North Carolina, USA. [3]Department of Cell Biology and Physiology, The University of North Carolina at Chapel Hill, Chapel Hill, North Carolina, USA. [4]Department of Microbiology and Immunology, University of Texas Medical Branch, Galveston, Texas, USA. [5]Department of Pathology, The University of North Carolina at Chapel Hill, Chapel Hill, North Carolina, USA. [6]Department of Internal Medicine I, J.W. Goethe University Hospital, Frankfurt, Germany. [7]Center for Integrated Protein Science Munich (CIPSM), Department of Life Sciences, Technical University Munich, Freising, Germany. [8]Department of Molecular and Cellular Biochemistry, Indiana University, Bloomington, Indiana, USA. [9]Department of Microbiology and Immunology, The University of North Carolina at Chapel Hill, Chapel Hill, North Carolina, USA. [10]Department of Genetics, The University of North Carolina at Chapel Hill, Chapel Hill, North Carolina, USA. [11]Department of Epidemiology, The University of North Carolina at Chapel Hill, Chapel Hill, North Carolina, USA. [12]School of Biology, Georgia Institute of Technology, Atlanta, Georgia, USA. [13]Parker H. Petit Institute for Bioengineering and Bioscience, Georgia Institute of Technology, Atlanta, Georgia, USA. [14]Severance Biomedical Science Institute, Yonsei University College of Medicine, Seoul, Korea. [15]Centre for Cancer Biology, SA Pathology, Adelaide, South Australia, Australia. Correspondence should be addressed to D.Y. (yamane@email.unc.edu) or S.M.L. (smlemon@med.unc.edu).

Received 31 March; accepted 23 May; published online 27 July 2014; doi:10.1038/nm.3610

these virus-host interactions in cell culture, we discovered that JFH1 differs from other HCV strains in its response to inhibitors of sphingolipid-converting enzymes. These initial observations led to experiments that show the HCV replicase to be exquisitely sensitive to endogenous lipid peroxidation, a feature lacking in the atypical JFH1 strain and other pathogenic RNA viruses. Our findings suggest that HCV possesses a unique capacity to sense lipid peroxides induced by infection and to respond to their presence by restricting viral RNA synthesis, thereby limiting virus replication and possibly facilitating virus persistence.

RESULTS

Sphingosine kinase-2 regulates HCV replication

We determined how inhibitors of sphingolipid-converting enzymes influence replication of three cell culture–adapted HCVs: H77S.3, a genotype 1a virus, N2, a genotype 1b virus, and HJ3-5, an intergenotypic chimera expressing the genotype 2a JFH1 replicase. To assess replication, we monitored *Gaussia princeps* luciferase (GLuc) produced by Huh-7.5 cells transfected with synthetic viral RNAs containing in-frame GLuc insertions[27] (**Fig. 1a**). Unexpectedly, the H77S.3/GLuc and HJ3-5/GLuc RNAs demonstrated contrary responses to many inhibitors, including, most notably, SKI, a sphingosine kinase (SPHK) inhibitor (**Fig. 1b** and **Supplementary Fig. 1a,b**). We also observed contrasting responses to sphingolipid supplementation (**Supplementary Fig. 1c**). SKI (1 μM) enhanced replication of H77S.3/GLuc and also N.2/GLuc by three- to sixfold but suppressed replication of HJ3-5/GLuc (**Fig. 1b,c**). These effects were evident within 48 h of exposure. We observed similar effects with viral RNAs lacking GLuc insertions: SKI enhanced H77S.3 protein expression tenfold while slightly suppressing HJ3-5 protein expression (**Fig. 1d**). Thus, changes in the cellular environment induced by SKI favor H77S.3 and N.2 replication and inhibit that of HJ3-5. These effects were not due to altered cell proliferation or viral RNA translation (**Supplementary Fig. 2a,b**). We observed similar results with autonomously replicating, subgenomic HCV RNAs ('replicons') in multiple cell types (**Supplementary Fig. 2c,d**).

SPHK is expressed as two isoforms[28], which we individually silenced by transfecting cells with gene-specific siRNAs. Partial type 2 SPHK (SPHK2) depletion enhanced replication of H77S.3/GLuc and N.2/GLuc, whereas SPHK1 depletion inhibited both viruses (**Fig. 1e,f**). In contrast, replication of HJ3-5/GLuc and cell culture–adapted JFH1 (JFH-QL/GLuc, **Fig. 1a**) viruses was increased following SPHK1 depletion and decreased after SPHK2 knockdown. Neither SPHK1 nor SPHK2 knockdown substantially affected cell proliferation (**Supplementary Fig. 2e**). Thus, SKI enhances replication of H77S.3/GLuc and N.2/GLuc by inhibiting SPHK2. Consistent with this, SKI preferentially inhibited SPHK2 in cell-free assays (**Supplementary Fig. 2f**) and demonstrated no activity against endogenous SPHK1 at low concentrations (≤2 μM) (**Supplementary Fig. 2g**). SKI did not act by regulating the intracellular abundance of sphingomyelin, cholesterol, triglyceride or lipid droplets, and sensitivity to SKI was not determined by the sphingomyelin binding domain of NS5B (**Supplementary Results** and **Supplementary Figs. 3** and **4**).

Lipid peroxidation is a key factor in SKI regulation of HCV

Polyunsaturated fatty acids (PUFAs) inhibit replication of genotype 1b HCV replicons by inducing lipid peroxidation[8,29]. Notably, although PUFAs such as arachidonic acid, docosahexaenoic acid or linoleic acid potently suppressed H77S.3/GLuc replication without affecting cell viability, HJ3-5/GLuc was highly resistant to this inhibitory effect (**Fig. 2a,b** and **Supplementary Fig. 5a,b**). Thus, PUFAs appear to phenocopy the effect of SPHK2 on HCV replication, suggesting that SPHK2 promotes lipid peroxidation. Consistent with this hypothesis, SKI completely abolished the inhibitory effects of PUFAs on H77S.3/GLuc and N.2/GLuc (**Fig. 2c**). SKI also lowered the intracellular abundance of malondialdehyde (MDA), a secondary product

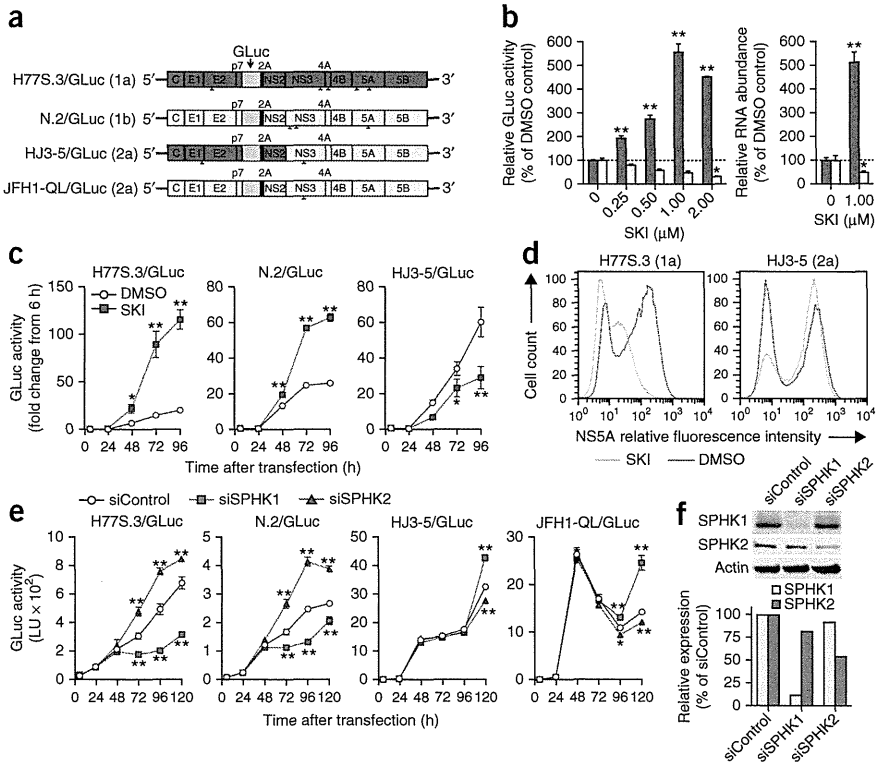

Figure 1 SKI enhances genotype 1 HCV replication while suppressing JFH1-based viruses by inhibiting SPHK2. (**a**) HCV RNA genomes that express GLuc fused to foot-and-mouth disease virus 2A autoprotease as part of the HCV polyprotein. Arrowheads indicate cell culture–adaptive mutations. (**b**) Left, dose-response effects of SKI on replication of H77S.3/GLuc (red) or HJ3-5/GLuc (blue) RNAs in Huh-7.5 cells. Right, effect of 1 μM SKI on replication of H77S.3 (red) or HJ3-5 (blue) RNAs. Data represent relative amounts of GLuc secreted between 48–72 h (left) or intracellular RNA levels at 72 h (right). $*P < 0.05$, $**P < 0.001$ by two-way ANOVA. (**c**) Effect of 1 μM SKI on GLuc activities of the indicated viruses presented as fold change from baseline (6 h). $*P < 0.05$, $**P < 0.001$ by two-way ANOVA. (**d**) Flow cytometric analysis of NS5A expression in Huh-7.5 cells electroporated with H77S.3 or HJ3-5 RNA and treated with 1 μM SKI or DMSO. (**e**,**f**) Effect of siRNAs targeting SPHK isoforms or nontargeting control siRNA on replication of different HCV RNAs (**e**) and protein abundance of each SPHK isoform (**f**). LU, light units. $*P < 0.05$, $**P < 0.01$ by two-way ANOVA. Results represent the mean ± s.e.m. from two independent (**b**,**c**,**d**) or triplicate (**e**) experiments.

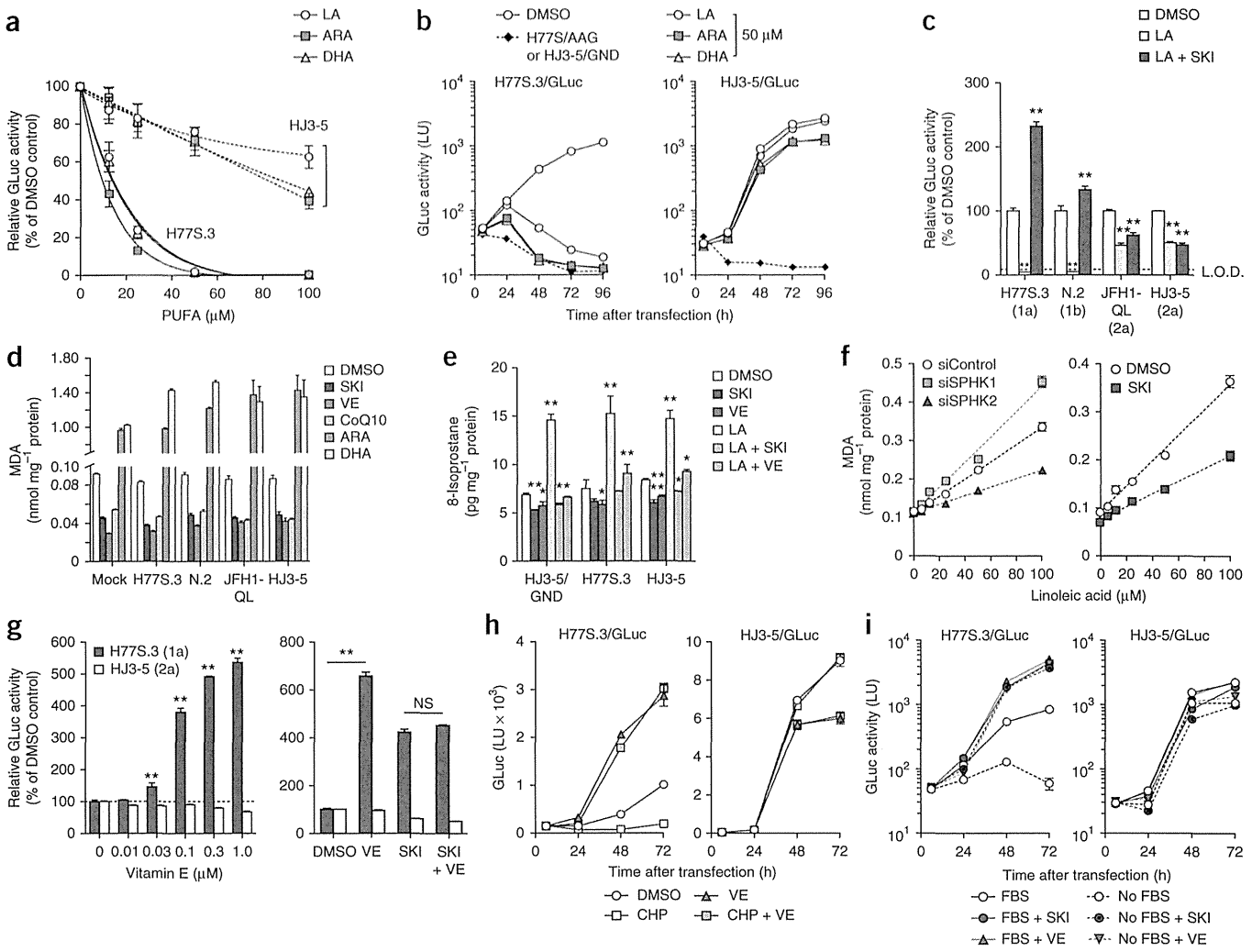

Figure 2 Differential regulation of HCV strains by SPHK2-mediated lipid peroxidation. (**a**) Dose-dependent effects of PUFAs on H77S.3/GLuc and HJ3-5/GLuc RNAs in Huh-7.5 cells. Data represent percentage secreted GLuc activity between 48–72 h relative to DMSO control. (**b**) Growth kinetics of H77S.3/GLuc and HJ3-5/GLuc RNAs in the presence of 50 μM PUFAs. Data are mean ± s.e.m. of GLuc activity in supernatant fluids of two replicate cultures. (**c**) Cells transfected with HCV RNAs encoding GLuc treated with DMSO, 100 μM linoleic acid (LA) or 100 μM linoleic acid plus 1 μM SKI. Data represent percentage secreted GLuc activity between 48–72 h relative to DMSO control. L.O.D., limit of detection. (**d**) Effect of 1 μM SKI, 1 μM vitamin E (VE), 100 μM CoQ10 or 50 μM arachidonic acid (ARA) or docosahexaenoic acid (DHA) on intracellular MDA abundance in cells transfected with the indicated HCV/GLuc RNAs at 72 h. MDA was significantly increased by PUFAs and reduced by SKI or lipophilic antioxidants ($P < 0.01$ by ANOVA). (**e**) Analysis of 8-isoprostane abundance in cells electroporated with the indicated HCV RNAs and grown in the presence of 1 μM SKI or vitamin E or of 50 μM linoleic acid with or without 1 μM SKI or vitamin E for 48 h. (**f**) Left, effect of siRNA targeting SPHK isoforms (**Fig. 1f**) on MDA accumulation after treatment with increasing concentrations of linoleic acid (6.25, 12.5, 25, 50, 100 μM) for 24 h. Right, MDA levels in Huh-7.5 cells treated with increasing concentrations of linoleic acid in the presence of DMSO or 1 μM SKI. (**g**) Effects of increasing concentrations of vitamin E (left) or 1 μM vitamin E alone or 1 μM vitamin E plus 1 μM SKI (right) on replication of H77S.3/GLuc and HJ3-5/GLuc RNAs. Data represent GLuc secreted between 48–72 h relative to DMSO control. NS, not significant. (**h**) GLuc secretion from Huh-7.5 cells transfected as in **a** and treated with 10 μM CHP with or without 10 μM vitamin E. (**i**) Influence of SKI or vitamin E (each 1 μM) on replication of H77S.3 and HJ3-5 viruses expressing GLuc in cells cultured in the presence or absence of 10% FBS. Data represent mean ± s.e.m. from two (**a–f,i**) or three (**g,h**) independent experiments. $^{*}P < 0.05$, $^{**}P < 0.01$ by two-way ANOVA.

of peroxidative degradation, in both HCV-infected and uninfected cells (**Fig. 2d**). SKI was as effective as the lipophilic antioxidants vitamin E (α-tocopherol) and coenzyme Q10 (CoQ10) in reducing MDA abundance and, like vitamin E and CoQ10, prevented large increases in lipid peroxidation induced by PUFAs (**Fig. 2d,e**). SKI also reduced both endogenous and PUFA-induced synthesis of 8-isoprostane, an alternative biomarker of lipid peroxidation (**Fig. 2e**). Conversely, RNAi-mediated depletion of SPHK1 increased the intracellular abundance of MDA in cells treated with increasing concentrations of linoleic acid, whereas SPHK2 knockdown, like SKI, reduced it (**Fig. 2f**). Thus, the contrasting effects of SPHK1 and SPHK2 on HCV replication may be explained by their opposing actions on peroxidation of endogenous PUFA. These results identify SPHK2 as a key mediator of lipid peroxidation.

Lipid-soluble antioxidants, including multiple forms of vitamin E (α-, *rac*-β- and γ-tocopherols), CoQ10 and butylated hydroxytoluene, enhanced H77S.3/GLuc replication in a concentration-dependent fashion, as described for a genotype 1b replicon[8], but suppressed HJ3-5/GLuc replication (**Fig. 2g** and **Supplementary Fig. 5c–e**). Notably, the effects of vitamin E and SKI on H77S.3/GLuc or N.2/GLuc replication were not additive (**Fig. 2g** and **Supplementary Fig. 5f**), suggesting

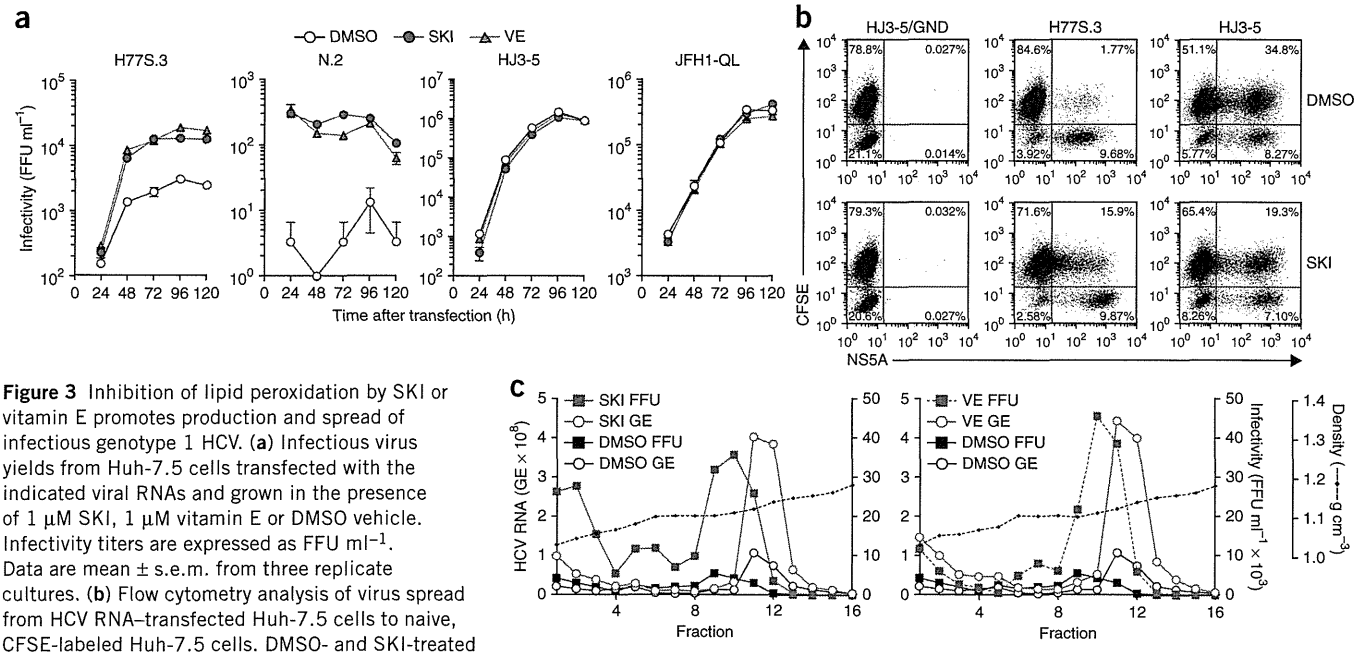

Figure 3 Inhibition of lipid peroxidation by SKI or vitamin E promotes production and spread of infectious genotype 1 HCV. (**a**) Infectious virus yields from Huh-7.5 cells transfected with the indicated viral RNAs and grown in the presence of 1 μM SKI, 1 μM vitamin E or DMSO vehicle. Infectivity titers are expressed as FFU ml^{-1}. Data are mean ± s.e.m. from three replicate cultures. (**b**) Flow cytometry analysis of virus spread from HCV RNA–transfected Huh-7.5 cells to naive, CFSE-labeled Huh-7.5 cells. DMSO- and SKI-treated cultures are shown for each transfected RNA. Percentages represent the percentage of all cells in each quadrant. $CFSE^{+}NS5A^{+}$ cells (upper right quadrant) are indicative of virus spread. (**c**) Buoyant density of H77S.3 virus particles released from H77S.3 RNA–transfected Huh-7.5 cells grown in 1 μM SKI (left) or 1 μM vitamin E (right) versus DMSO control. Fractions from isopycnic iodixanol gradients were assayed for infectious virus (FFU) or HCV RNA (GE, genome equivalents). Data are representative of two independent experiments.

that both act via a common antioxidant mechanism. Antioxidants that are not soluble in lipids, such as ebselen and *N*-acetylcysteine, as well as the NADPH oxidase inhibitor diphenyleneiodonium, had very little effect on H77S.3/GLuc replication (**Supplementary Fig. 5g**), whereas cumene hydroperoxide (CHP), a lipophilic oxidant, suppressed H77S.3/GLuc replication in a vitamin E–reversible fashion (**Fig. 2h**). FBS contains substantial quantities of lipophilic antioxidants[8]. H77S.3/GLuc replication was 20-fold lower in FBS-free cultures but was enhanced 100-fold with either SKI or vitamin E (**Fig. 2i**). HJ3-5/GLuc replication was relatively unimpaired in FBS-free medium. Collectively, these data provide evidence that endogenous lipid peroxidation restricts H77S.3/GLuc and N.2/GLuc replication, whereas the JFH1 replicase is resistant to both endogenous and chemically induced lipid peroxidation.

Endogenous lipid peroxidation restricts infectious HCV yield

Both SKI and vitamin E induced a tenfold increase in the yield of infectious virus released by H77S.3 RNA–transfected cells, reaching ~20,000 focus-forming units per milliliter (FFU ml^{-1}) (**Fig. 3a** and **Supplementary Fig. 6a**). Infectious N.2 virus yields were increased up to 100-fold (**Fig. 3a**). SKI also enhanced virus spread when we cultured H77S.3 RNA–transfected cells with nontransfected carboxyfluorescein succinimidyl ester (CFSE)-labeled cells (**Fig. 3b**). In contrast, neither SKI nor vitamin E enhanced infectious yields of JFH1-QL or HJ3-5 viruses (**Fig. 3a**), whereas SKI reduced the spread of HJ3-5 virus by >40% (**Fig. 3b**).

HCV particles produced in cell culture have heterogeneous buoyant densities[30]. However, most H77S.3 particles produced in the absence of SKI or vitamin E banded between 1.12 and 1.14 g cm^{-3} in isopycnic gradients, with peak infectivity banding between 1.10 and 1.11 g cm^{-3} (**Fig. 3c**). Neither SKI nor vitamin E altered the distribution of RNA-containing or infectious particles in gradients, but they substantially increased the abundance of both (**Fig. 3c**). SKI and vitamin E also caused modest increases in the maximum specific infectivity of virus particles (**Supplementary Fig. 6b**). Thus, SKI and vitamin E act primarily on replication of H77S.3 RNA, leading to enhanced production of infectious virus.

Lipid peroxidation restricts HCV in primary hepatocytes

To assess replication of wild-type HCV genomes possessing no cell culture–adaptive mutations, we inserted a GLuc sequence into infectious molecular clones of H77c and N[31,32]. Both H77c/GLuc and N/GLuc RNAs produced more GLuc in electroporated cells than RNA with a lethal mutation in NS5B, H77c/GLuc-AAG (**Fig. 4a**). GLuc secretion produced by either RNA was eliminated by direct-acting antivirals (DAA) targeting NS5B, confirming it represents genuine viral replication. Treatment with either SKI or vitamin E markedly increased GLuc production, whereas linoleic acid decreased GLuc secretion to background (**Fig. 4a**). Moreover, the inhibitory effect of linoleic acid was reversed by cotreatment with SKI or vitamin E. In contrast, GLuc production by wild-type JFH1/GLuc was not affected by SKI, vitamin E or linoleic acid (**Fig. 4b**). Thus, endogenous lipid peroxidation is a critical restriction factor for H77c and N viruses but not for wild-type JFH1.

To assess the effects of SKI and vitamin E on HCV replication in cells that are closely related to those naturally infected by the virus, we studied primary human fetal hepatoblasts (HFHs). SKI and vitamin E significantly increased replication of the H77S.3/GLuc reporter virus in HFHs ($P < 0.0001$ by two-way analysis of variance (ANOVA) with Holm-Sidak correction for multiple comparisons), sustaining GLuc expression for 7 d after low-multiplicity infection (**Fig. 4c,d**). In contrast, linoleic acid suppressed H77S.3 infection in HFHs in a vitamin E–reversible manner (**Fig. 4d**). Whereas H77S.3/GLuc replicated efficiently in the presence of vitamin E or SKI, HJ3-5/GLuc replication was inhibited by SKI ($P < 0.001$ by two-way ANOVA with Holm-Sidak correction for multiple comparisons) and to a lesser extent by vitamin E

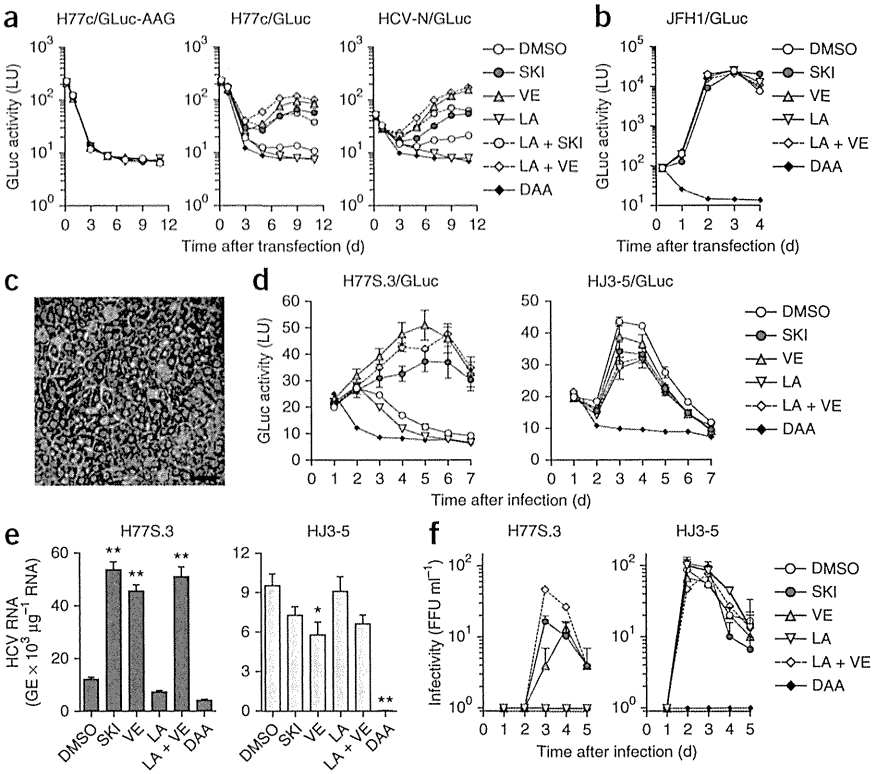

Figure 4 Lipid peroxidation regulates wild-type HCV replication and represses cell culture–adapted virus in primary human liver cultures. (**a**) Effects of SKI or vitamin E (each 1 μM), linoleic acid (20 μM), linoleic acid + SKI, linoleic acid + vitamin E or a DAA (MK-0608, 10 μM) on replication of wild-type H77c/GLuc or HCV-N/GLuc RNAs or a replication-defective control (H77c/GLuc-AAG) in Huh-7.5 cells. (**b**) Effects of SKI, vitamin E and linoleic acid (as in **a**) on replication of wild-type JFH1/GLuc RNA. DAA, PSI-6130 (10 μM). (**c**) Phase contrast microscopy of fetal hepatoblasts at 3 d. Scale bar, 50 μm. (**d**) HFHs infected with H77S.3/GLuc or HJ3-5/GLuc viruses (multiplicity of infection (MOI) = 0.001) in HFH medium containing SKI or vitamin E (each 1 μM), linoleic acid (50 μM), linoleic acid + vitamin E or a DAA (MK-0608 or PSI-6130, 10 μM) and assayed for GLuc. Results represent mean ± s.e.m. from three replicate cultures with cells from two donors. $P < 0.0001$ for SKI, VE and LA + VE compared to DMSO at 5–7 d, two-way ANOVA with Holm-Sidak correction for multiple comparisons. (**e**) HFHs infected with H77S.3 or HJ3-5 (MOI = 0.01) and treated as in **d**. Cell-associated viral RNA was quantified by quantitative RT-PCR (qRT-PCR) at 5 d (*$P < 0.05$, **$P < 0.001$ by two-way ANOVA. GE, genome equivalent. (**f**) Infectious virus released from H77S.3 or HJ3-5 virus–inoculated HFHs (MOI = 0.01). Virus was quantified by FFU assay. Results represent mean ± s.e.m. from three replicate cultures.

($P < 0.05$) (**Fig. 4d**). We observed similar results in cells infected with H77S.3 or HJ3-5 viruses lacking a GLuc insertion (**Fig. 4e**). We detected production of infectious H77S.3 virus in HFH cultures only in the presence of vitamin E or SKI and found that infectious HJ3-5 yields were not enhanced by either treatment (**Fig. 4f**). Whereas the disruption of innate immune responses is known to promote HCV replication in HFHs[33], neither SKI nor vitamin E reduced Sendai virus activation of the interferon-β promoter (**Supplementary Fig. 7**). Thus, SKI and vitamin E do not promote H77S.3 replication in HFHs by blocking activation of the interferon response to virus infection.

Lipid peroxidation reduces the EC_{50} of direct antivirals

Both SKI and vitamin E treatment increased the area occupied by the membranous web in H77S.3-infected cells (**Fig. 5a,b**) without altering the morphology of double-membrane vesicles, which are the likely site of genome replication[14]. Increased lipid peroxidation reduced the area occupied by the membranous web, whereas the HJ3-5 membranous web was insensitive to changes in lipid peroxidation.

Reverse molecular genetic studies involving exchanges between the H77S.3 and JFH1 genomes suggested that the peroxidation resistance phenotype of JFH1 involves multiple nonstructural proteins within the replicase (**Supplementary Results** and **Supplementary Fig. 8**). Consistent with this, we observed an unexpected increase in the 50% effective concentration (EC_{50}) of DAAs targeting the NS3-4A protease (a noncovalent complex of NS3 and its cofactor, NS4A) and NS5B polymerase after suppressing endogenous lipid peroxidation in H77S.3/GLuc-infected cells (**Fig. 5d,e** and **Supplementary Fig. 9a–c**). Both SKI and vitamin E masked the antiviral effects of PSI-6130, a potent NS5B inhibitor (**Fig. 5c**), in part owing to an increase in its EC_{50} from 3.49 μM (95% confidence interval (CI) 2.48–4.89) to 6.22 μM (4.43–8.72) and 8.46 μM (7.60–9.44), respectively (**Fig. 5d**). SKI and vitamin E also increased the EC_{50} of MK-7009, an inhibitor of the NS3-4A protease, from 0.488 nM (95% CI 0.411–0.578) to 1.45 nM (1.23–1.72) and 1.90 nM (1.64–2.22), respectively (**Fig. 5e**). The EC_{50} values of other inhibitors targeting NS3-4A (boceprevir) and NS5B (HCV-796 and MK-0608) were similarly increased against H77S.3/GLuc by SKI and vitamin E, but neither SKI nor vitamin E significantly altered the EC_{50} of SCY-635, cyclosporine A, compound 23 or a locked nucleic acid–modified oligonucleotide complementary to miR-122 (anti-miR-122), inhibitors targeting essential HCV host factors, or interferon-α (**Fig. 5f,g** and **Supplementary Fig. 9d–g**). In contrast, SKI and vitamin E caused no change in the EC_{50} of any antiviral against HJ3-5/GLuc (**Fig. 5d,g** and **Supplementary Fig. 9a–f**), indicating that vitamin E and SKI do not impair cellular uptake or metabolism of DAAs. These changes in the EC_{50} against H77S.3/GLuc thus probably reflect altered affinity of the DAAs for NS3-4A and NS5B, suggesting that peroxidation modulates the conformation of these replicase proteins.

Resistance to lipid peroxidation maps to NS4A and NS5B

TNcc is a recently described genotype 1a virus with eight cell culture–adaptive mutations that replicates almost as well as JFH1 in Huh-7.5 cells[34]. Notably, we found it completely resistant to lipid peroxidation (**Fig. 6a** and **Supplementary Fig. 10a**). We introduced all eight TNcc mutations into H77S.3 to determine whether they would confer peroxidation resistance. This RNA (H77S.3/$GLuc_{8mt}$) failed to replicate, but removal of a key H77S.3 adaptive mutation (S2204I in NS5A)[12] restored low-level replication. The resulting virus, H77S.3/$GLuc_{IS/8mt}$, was resistant to lipid peroxidation (**Fig. 6a** and **Supplementary Fig. 10b**). Continued passage of cells infected with H77S.$3_{IS/8mt}$ resulted in the emergence of viruses carrying additional mutations in NS4B (G1909S), NS5A (D2416G) and NS5B (G2963D) that together enhanced replication by 850-fold (**Supplementary Results** and **Supplementary Fig. 11**). The NS4B G1909S mutation

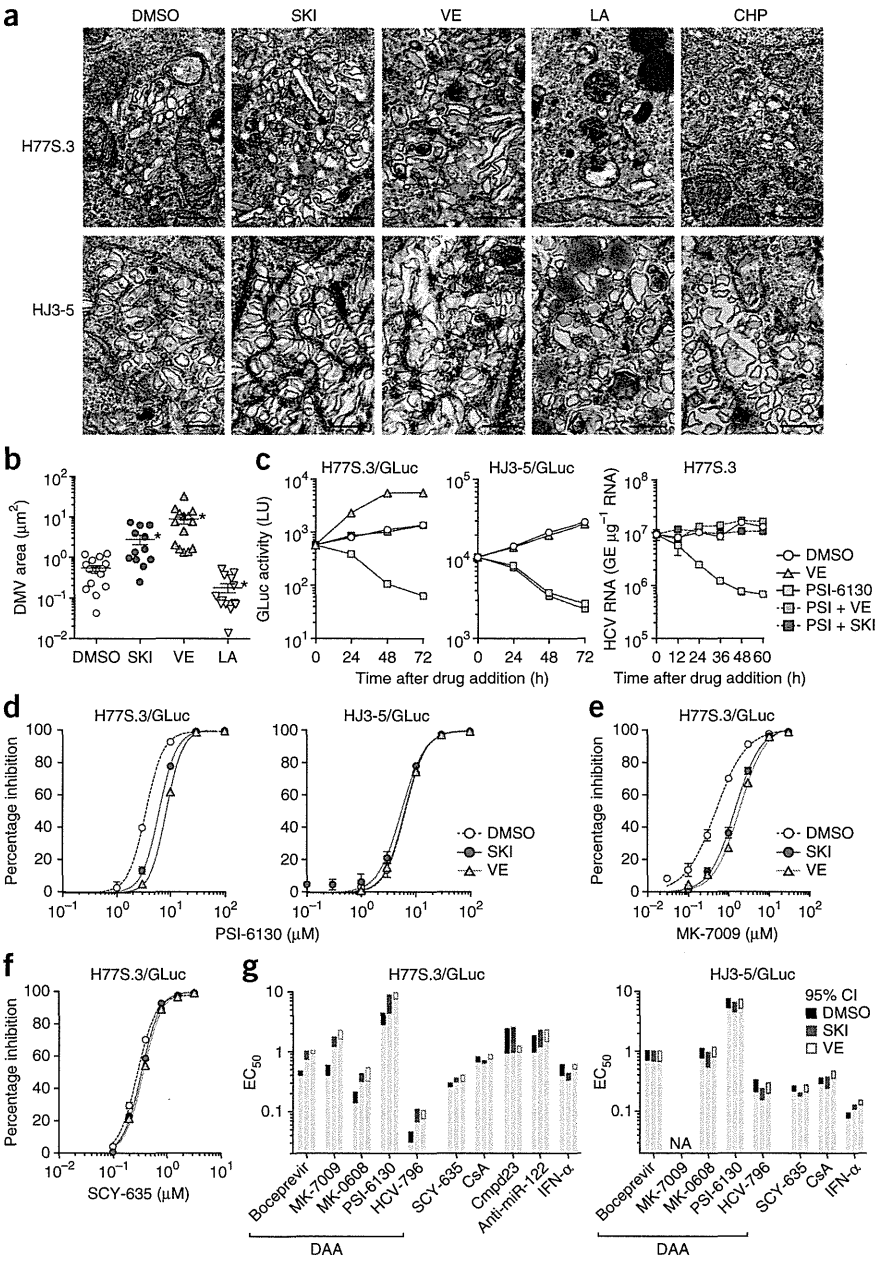

Figure 5 Lipid peroxidation reduces HCV-induced membranous web abundance and alters the EC_{50} of DAAs. (**a**) Transmission electron microscopic images of the membranous web in Huh-7.5 cells electroporated with H77S.3 or HJ3-5 RNA and treated with DMSO, SKI (1 μM), vitamin E (1 μM), linoleic acid (50 μM) or CHP (10 μM). Images shown are representative of 10 different microscopic fields. Scale bars, 500 nm. (**b**) Quantitation of area occupied by double-membrane vesicles (DMV) within individual cells infected with H77S.3 virus and treated with SKI, vitamin E or linoleic acid as in **a**. $^*P \leq 0.002$ versus DMSO by two-sided Mann-Whitney *U* test. (**c**) The effect of SKI and vitamin E on the antiviral effect of PSI-6130 against H77S.3/GLuc replication. Left and middle, GLuc produced from Huh-7.5 cells transfected with H77S.3/GLuc or HJ3-5/GLuc RNA 7 d prior to treatment with DMSO, 10 μM PSI-6130, 1 μM vitamin E or both PSI-6130 and either SKI or vitamin E. Right, Cell-associated HCV RNA in similarly treated cells transfected with H77S.3 RNA. Results represent mean ± s.e.m. from two (left, middle) or three (right) replicate cultures. (**d**) Inhibition of H77S.3 (left) and HJ3-5 (right) replication by the NS5B inhibitor PSI-6130 in the presence of SKI or vitamin E (each 1 μM) or DMSO vehicle, assessed by quantifying GLuc secreted 48–72 h after drug addition. Results represent mean ± s.e.m. of two replicate cultures. (**e**,**f**) Inhibition of H77S.3 replication by MK-7009, an NS3-4A inhibitor, (**e**) and SCY-635, a host-targeting cyclophilin inhibitor (**f**). Results represent mean ± s.e.m. of triplicate cultures. (**g**) EC_{50} values of direct-acting versus indirect-acting antivirals against H77S.3 (left) and HJ3-5 (right) viruses in the presence of SKI or vitamin E (each 1 μM). Assays were carried out as in **d**–**f**. Colored bars represent limits of the 95% CI of EC_{50} values calculated from Hill plots. NA, not measureable owing to poor antiviral activity; IFN-α, interferon-α; CsA, cyclosporine A; Cmpd23, compound 23. Additional details are shown in **Supplementary Figure 9**.

compensated for the negative effects on replication of TNcc mutations placed into the H77S.3 background (**Fig. 6b**). When we introduced all three additional mutations (G1909S, D2416G and G2963D) into $H77S.3/GLuc_{IS/8mt}$, the resulting virus (designated H77D) produced infectious virus yields comparable to those of HJ3-5 or JFH1-QL, which were not increased by vitamin E supplementation (**Fig. 6b**). Notably, the EC_{50} of DAAs against H77D virus was not altered by SKI or vitamin E (**Fig. 6d** and **Supplementary Fig. 9h**).

Introducing the G1909S mutation into $H77S.3/GLuc_{IS}$ ($H77S.3/GLuc_{IS/GS}$) did not confer peroxidation resistance (**Fig. 6a**). However, its compensatory effect on the TNcc-derived mutations allowed us to identify the A1672S mutation (in NS4A) from TNcc as essential for peroxidation resistance and to show that TNcc-derived mutations in NS3 and NS4B were not required for this phenotype (**Fig. 6a**). TNcc mutations in NS5B (D2979G, Y2981F and F2994S) were essential for replication of peroxidation-resistant virus, but neither these nor A1672S (in NS4A) alone conferred peroxidation resistance (**Supplementary Fig. 10c**). Thus, mutations in both NS4A and NS5B are required for genotype 1a peroxidation resistance. These mutations are within or in close proximity to the transmembrane domains of these proteins (**Fig. 6c**), consistent with direct involvement of these residues in resistance to lipid peroxidation.

Regulation by lipid peroxidation is unique to HCV

In addition to replication of genotypes 1a (H77S.3) and 1b (HCV-N.2) (**Figs. 2c** and **3a**), replication of HCV genotypes 2a (JFH-2), 3a (S52) and 4a (ED43) was enhanced by treatment with SKI or vitamin E and inhibited by CHP-induced lipid peroxidation (**Fig. 6e**). JFH1 is thus unique among wild-type HCV strains in its resistance to lipid peroxidation.

As with HCV, the genomes of other positive-strand RNA viruses are synthesized by replicase complexes that assemble in association with cytoplasmic membranes and are thus at risk for damage due to lipid peroxidation. Yet, like replication of JFH1, the replication of other